

## Article

# The Future of Last-Mile Delivery: Lifecycle Environmental and Economic Impacts of Drone-Truck Parallel Systems

Danwen Bao <sup>1,2</sup> , Yu Yan <sup>1,\*</sup> , Yuhang Li <sup>3</sup>  and Jiajun Chu <sup>1</sup>

<sup>1</sup> College of Civil Aviation, Nanjing University of Aeronautics and Astronautics, Nanjing 210016, China; baodanwen@nuaa.edu.cn (D.B.); harrychujiajun@nuaa.edu.cn (J.C.)

<sup>2</sup> State Key Laboratory of Air Traffic Management System, Nanjing 211106, China

<sup>3</sup> School of Aeronautic Science and Engineering, Beihang University, Beijing 100191, China; ffflora@buaa.edu.cn

\* Correspondence: yanyu816@nuaa.edu.cn

**Abstract:** With rapid advancements in unmanned aerial vehicle (UAV) technology, its integration into logistics operations has emerged as a promising solution for improving efficiency and sustainability. Among the emerging solutions, a collaborative delivery model involving drones and trucks addresses last-mile delivery challenges by leveraging the complementary strengths of both modes of transport. However, evaluating the environmental and economic impacts of this transportation mode requires a systematic framework to capture its unique characteristics and minimize environmental impacts and costs. This paper investigates the Parallel Drone Scheduling Traveling Salesman Problem (PDSTSP) to evaluate the environmental and economic sustainability of a collaborative drone-truck delivery system. Specifically, a mathematical model for this delivery system is developed to optimize joint delivery operations. Environmental impacts are assessed using a comprehensive Life Cycle Assessment (LCA), including emissions and operational noise, while a Life Cycle Cost Analysis (LCCA) quantifies economic performance across five cost dimensions. Sensitivity analysis explores factors such as delivery density, traffic congestion, and wind conditions. Results show that, compared to the electric vehicle fleet, the proposed model achieves an approximate 20% reduction in carbon emissions, while delivering a 20–30% cost reduction relative to the fuel truck fleet. Drones' efficiency in short-distance deliveries alleviates trucks' load, cutting environmental and operational costs. This study offers practical insights and recommendations for implementing drone-truck parallel delivery systems, particularly in high-demand density areas.



Academic Editor: Pablo Rodríguez-González

Received: 10 December 2024

Revised: 7 January 2025

Accepted: 12 January 2025

Published: 14 January 2025

**Citation:** Bao, D.; Yan, Y.; Li, Y.; Chu, J. The Future of Last-Mile Delivery: Lifecycle Environmental and Economic Impacts of Drone-Truck Parallel Systems. *Drones* **2025**, *9*, 54. <https://doi.org/10.3390/drones9010054>

**Copyright:** © 2025 by the authors. Licensee MDPI, Basel, Switzerland. This article is an open access article distributed under the terms and conditions of the Creative Commons Attribution (CC BY) license (<https://creativecommons.org/licenses/by/4.0/>).

## 1. Introduction

Driven by the rapid expansion of e-commerce and evolving consumer demands, last-mile logistics has undergone significant advancements. Among these, autonomous vehicles, especially drones, stand out prominently [1]. Drones offer swift and reliable services while promoting environmental sustainability by reducing emissions [2]. In 2019, the European Union introduced Regulations 2019/947 and 2019/945, which detail requirements for drone operations and remote pilots, including beyond visual line of sight (BVLOS) delivery under risk assessments and compliance conditions. In 2020, the Federal Aviation Administration issued regulations on UAV flight rules, airspace, pilot licenses, and registration requirements. In 2023, China enacted its first comprehensive interim regulation to govern drone operations. These regulatory developments have

spurred the commercialization of drones, with major companies exploring their logistics applications. For instance, Amazon focused on testing drones for the last-mile delivery of small parcels [3], while Alibaba has tested UAV delivery services in cities such as Beijing and Shanghai. Meituan also launched a commercial drone route in Shanghai in 2023. The potential for drone development is immense, with the civil UAS market expected to grow from USD 4.9 billion in 2019 to around USD 14.3 billion by 2028 [4].

As electrically powered vehicles, drones offer energy efficiency and environmental benefits [5]. Unlike traditional ground vehicles, drones navigate direct routes, bypassing obstacles and congestion, which speeds up deliveries. A comparison shows that drone delivery costs for a standard shoebox are only USD 0.05 per mile, significantly lower than the costs of ground delivery, estimated to be 40 to 100 times higher [6]. Moreover, drones support sustainable logistics by reducing emissions, particularly in densely populated urban areas. However, in sparsely populated regions, such as towns and villages, electric trucks are more energy-efficient than drones [7].

The environmental and economic impacts of many products often concentrate in the production and disposal phases rather than the use phase [8]. Life Cycle Assessment (LCA) provides a comprehensive framework for evaluating impacts across a product's lifecycle, from raw material extraction to end-of-life disposal. While drones can offer environmental benefits, their advantages are not universally applicable. Ground transportation can outperform drones in lifecycle emissions, as drones consume more energy in adverse conditions, such as headwinds, increasing CO<sub>2</sub>e emissions [9,10]. Advances in drone automation and logistics optimization, however, present significant opportunities to reduce emissions and improve cost-efficiency [11].

Despite their advantages in flexibility [12], drones face limitations, such as restricted payload capacity and battery life, which limit their range and operational duration [13]. In contrast, trucks offer larger payloads and longer travel distances, making them better suited for bulk transportation. This complementary relationship suggests that integrating drones and trucks into a parallel transportation model can enhance last-mile logistics without requiring complex synchronization [14].

However, while there is growing interest in drone logistics, quantitative studies evaluating their environmental and economic sustainability remain limited. As a result, the overall impacts of this parallel transportation system are not well understood, particularly from the perspectives of governments and logistics operators. Therefore, two key challenges need to be considered as follows:

- Challenges from government management: Governments need to systematically quantify the environmental impacts of the system. This will enable accurate assessments, helping to identify potential issues. It will also support the formulation of targeted policies and standards for effective environmental management and regulation;
- Challenges from operations management: Operators need to quantify long-term costs. Establishing such a system involves significant investment in high-cost equipment, as well as long-term operational and maintenance expenses. Therefore, a comprehensive understanding of these costs is essential to help operators evaluate the feasibility and economic viability of the investment.

To address these challenges, this study systematically evaluates a parallel transportation system combining drones and ground vehicles. This study makes the following key contributions:

- Insights for sustainable logistics: It compares drone-truck parallel systems with traditional truck-based systems, highlighting their environmental and economic advantages. These insights provide recommendations for regulatory and operational strategies;

- Comprehensive sustainability assessment: By integrating LCA and Life Cycle Cost Analysis (LCCA), it assesses both environmental and economic sustainability. Specifically, a quantitative noise analysis is introduced for the operation phase, offering a more comprehensive evaluation of environmental impacts. Additionally, a detailed cost framework is developed, categorizing costs into five distinct categories, and applying the net present value (NPV) method for long-term economic assessments;
- Exploring critical factors: A sensitivity analysis is conducted to investigate the effects of critical factors, such as delivery density, traffic conditions, and wind speed on system performance across two sets of environmental and economic conditions.

This paper is organized as follows: Section 2 provides a literature review. Section 3 presents the problem statement, outlining key assumptions and the mathematical model. Section 4 describes the LCA and LCC models, focusing on their structure and components. Section 5 explains the optimization algorithms implemented. Section 6 discusses the experimental design, including the setup, parameters, and analyzed scenarios, and presents the results, highlighting the outcomes and their implications. Finally, Section 7 concludes with key findings and recommendations for future research and policy development.

## 2. Literature Review

This section reviews relevant studies on drone and truck transportation systems, with a primary focus on three aspects: drone-truck transportation models, environmental impacts, and economic benefits.

### 2.1. Developments in Drone-Truck Transportation Models

In recent years, truck-drone integrated delivery systems have emerged as a promising logistics model, attracting significant attention and experiencing rapid development. The integration of drones with trucks optimizes delivery routes, enhances efficiency, and reduces both carbon emissions and costs.

The Flying Sidekick Traveling Salesman Problem (FSTSP), introduced by [15], is one of the earliest and most influential models in truck-and-drone collaborative delivery systems. This model pairs a truck with a single drone to optimize delivery routes by balancing their respective operations. Formulated as a mixed-integer linear programming (MILP) problem, it serves as the foundation for subsequent studies that refine truck-drone collaboration. Ref. [16] extended this work with the Traveling Salesman Problem with Drone (TSP-D), where the drone returns to its launch point after completing deliveries. Ref. [17] improved the model using dynamic programming techniques, enabling them to handle instances with up to 20 nodes and reducing computational time. Ref. [18] introduced the Traveling Salesman Problem with Multiple Drones (TSP-MD), equipping the truck with multiple drones, each serving different customer locations. In a further refinement, ref. [19] developed the Multiple-FSTSP, considering drones with varying specifications (e.g., speed and payload capacity), allowing for more realistic operational modeling. Ref. [20] proposed a heuristic algorithm for the Multi-Point Delivery FSTSP, demonstrating superior performance in experiments. Ref. [21] used data science and machine learning to classify customers in the FSTSP, improving solution quality through new features and classification methods.

Building on the FSTSP, several variants of the problem have been developed. Ref. [15] introduced the concept of PDSTSP, pioneering a preliminary scheduling algorithm for routing optimization in this model. Building on this, ref. [22] further improved the route planning algorithm, employing a MILP approach to optimize the joint delivery paths of drones and trucks. Ref. [23] addressed the multi-objective optimization problem, improving the system's delivery efficiency and cost-effectiveness through a multi-objective genetic algorithm (MOGA). Ref. [24] proposed a task allocation model based on a heuristic algorithm

for the task scheduling problem in truck-drone parallel transportation systems. Ref. [25] presented an improved variable neighborhood search for the parallel drone scheduling traveling salesman problem, demonstrating its effectiveness through extensive experiments. Ref. [26] formulated the minimum-cost parallel drone scheduling vehicle routing problem (PDSVRP), developed a destroy-and-repair algorithm, and verified its optimization performance through experiments, finding new optimal solutions across multiple instances and significantly enhancing the efficiency of truck-drone collaborative delivery. Ref. [27] proposed the parallel drone scheduling multiple traveling salesman problem (PDSM-TSP) and developed a hybrid metaheuristic algorithm combining iterative local search and dynamic programming, with experimental results confirming its effectiveness.

As research progressed, attention shifted to more complex variants, with the Multi-Visit Truck-and-Drone Routing Problem (TDTLP) emerging as a key example. Introduced by [28], the TDTLP extends the FSTSP by incorporating multiple visits to customer locations, requiring effective coordination between the truck and drone. Building on this, several studies have further refined the TDTLP by considering various operational constraints and drone behaviors. For instance, refs. [29,30] focused on single-truck, single-drone routing problems under realistic logistical constraints, providing insights for more complex multi-visit scenarios. Several studies further extended the TDTLP to multi-truck and multi-drone systems, such as those by [31,32], which optimized coordination across multiple vehicles and drones for large-scale hybrid delivery systems. Ref. [33] proposed a MILP model and a branch-and-bound algorithm for the TDTLP, demonstrating superior solution efficiency and quality in experiments compared to existing methods.

## 2.2. Environmental Impact of Drone-Truck Transportation

Life Cycle Assessment (LCA) has been widely applied to evaluate the environmental impacts of drones across manufacturing, operation, and disposal stages. Recent studies have shown that the energy and materials consumed during the manufacturing process of drones have a significant environmental impact. Ref. [9] used LCA to assess emissions of drones operating from fixed warehouses, demonstrating that drones outperform traditional fuel trucks in terms of emissions when transport weight and distance are optimized. However, their overall emissions surpassed those of trucks when the latter had fewer delivery tasks. Ref. [5] utilized GIS data and field land-use data to compare the environmental impacts of drones and traditional trucks, noting that drones are advantageous over shorter distances, while trucks outperform drones over longer ranges. Ref. [34] examined the life cycle environmental impact of drone delivery systems with multiple intermediate warehouses, finding small drones more environmentally favorable than both electric and diesel vehicles, while large drones exhibited higher emissions. Ref. [35] compared the emissions of motorcycles and drones in pizza delivery systems and found that drones performed exceptionally well in terms of global warming potential, especially in urban environments, with emissions much lower than traditional delivery methods. Similarly, ref. [36] conducted a comparable study, showing that drones had lower emissions under high load conditions than ground vehicles, but higher emissions than electric vehicles. Ref. [7] analyzed drones' energy consumption, finding that drones generally have higher energy consumption than traditional trucks in dense areas, particularly during flight, where drones' energy consumption exceeded that of fuel trucks and electric vehicles.

In addition to environmental impacts, the noise generated during drone operations has garnered widespread attention. Ref. [37] developed a noise assessment method based on virtual flight, using Gaussian beam tracking technology to simulate the noise impact of drones and urban air mobility vehicles. Ref. [38] proposed a modeling framework to establish best practices for drone operations to minimize noise disruption to communities.

Ref. [39] conducted experiments using flight simulations and noise assessment platforms, finding that reducing drone flight speed and payload could effectively reduce noise impact, and that ground vegetation also played a significant role in noise attenuation. Ref. [40] measured the noise levels of different types of drones through flight tests and recommended establishing standardized drone noise measurement methods to enhance public acceptance of drone deliveries. Ref. [41] conducted a simulation analysis of noise hotspots in urban environments caused by drone delivery queues, proposing the FairNoise A\* algorithm, which balances noise distribution while minimizing the impact on environmental fairness.

### 2.3. Economic Impact of Drone-Truck Transport

The economic performance of drone-truck transportation has become a focal area of research. Refs. [22,42] conducted preliminary analyses of drone delivery economics, albeit excluding labor costs, which limited the comprehensiveness of the cost estimates. Ref. [43] explored the impact of battery capacity on the economics of drones, noting that operational costs for drones are expected to decrease significantly with advancements in battery technology. Additionally, optimizing the scale of the drone fleet will help improve delivery efficiency. Ref. [24] emphasized the critical role of operational costs in the overall economics, suggesting that equipping each truck with multiple drones could significantly enhance the system's economic performance. Ref. [44] validated this viewpoint, emphasizing the core importance of cost control in the optimization of transportation systems. Ref. [45] conducted a detailed analysis of capital expenditures and operational costs for drones in food delivery, noting that with the continuous development of drone technology, costs are expected to decline significantly. Ref. [46] summarized the current state of drone economics in last-mile delivery systems through a literature review, pointing out that current research has not fully covered the economic feasibility of drones, particularly in terms of life cycle cost assessments, which remain an area needing further improvement. Additionally, ref. [11] used total cost of ownership (TCO) to evaluate the economic sustainability of combining trucks and drones in last-mile delivery systems. The results indicated that the costs are highly influenced by the level of automation of the drones.

### 2.4. Current Status Summary

Most studies focus on FSTSP, where drones take off from trucks, complete delivery, and return while trucks continue their tasks. This approach suits scenarios where distribution centers are far from customers. However, as [47] noted, in urban areas with small, nearby distribution centers, direct drone deliveries are more feasible. The parallel operation of drones and trucks enables more flexible task allocation, without requiring synchronization protocols. This simplifies implementation for logistics providers, as tasks can be assigned based on each mode's strengths. In last-mile delivery, drones bypass traffic to deliver directly to customers, while trucks manage broader distribution, making the system ideal for dense urban environments.

Although existing research largely examines the environmental and economic impacts of collaborative truck-drone models, there is limited exploration of the practical effects and comprehensive impacts of drone-truck parallel systems. In terms of environmental analysis, many studies often emphasize emissions while overlooking factors like noise pollution. In economic analysis, current studies often focus only on direct costs, neglecting key factors such as environmental costs and additional operational costs. This limitation leads to the need for comprehensive evaluations of truck-drone parallel transportation to address both environmental sustainability and economic feasibility.

### 3. Problem Statement

This section defines the transportation model considered in this study and outlines the relevant key conditions and constraints. It provides a detailed description of two transportation modes: the parallel transportation fleet composed of trucks and drones, and the traditional ground transportation fleet. The model is then mathematically formulated, providing the basis for subsequent analysis.

#### 3.1. Definition and Assumption

In this paper, two transportation modes are considered: (1) a fleet consisting of electric or fuel vehicles, and (2) a parallel transportation fleet consisting of drones and a ground vehicle. For modeling these two modes of transportation, the following key conditions are established:

- (1) Simultaneous or independent operations: Trucks and UAVs are allowed to depart from and return to the depot either simultaneously or independently. The total completion time is defined as the duration from the departure of the first vehicle (either a truck or drone) to the return of the last vehicle to the depot;
- (2) Service node coverage: All customer demands must be fully met, with each customer being served exactly once by either trucks or a drone. Redundant or duplicate servicing is not permitted;
- (3) Parallel service: Drones and trucks operate concurrently, allowing each to serve different customers simultaneously. This collaborative approach enhances overall transportation efficiency by leveraging their complementary capabilities;
- (4) Delivery path strategies: Trucks complete deliveries for all assigned parcels before returning to the depot, while drones return to the depot for replenishment immediately after completing each delivery. This operational mode allows drones to execute frequent, short round trips, maximizing their responsiveness to individual delivery tasks;
- (5) Single depot: All transportation modes, including drones, fuel trucks, and electric vehicles, are assumed to originate and conclude their operations at the same depot.

Figure 1 illustrates the two transportation modes analyzed in this study, highlighting that all transportation modes depart from and return to the same fixed depot, which serves as the starting and ending point throughout the entire operation.

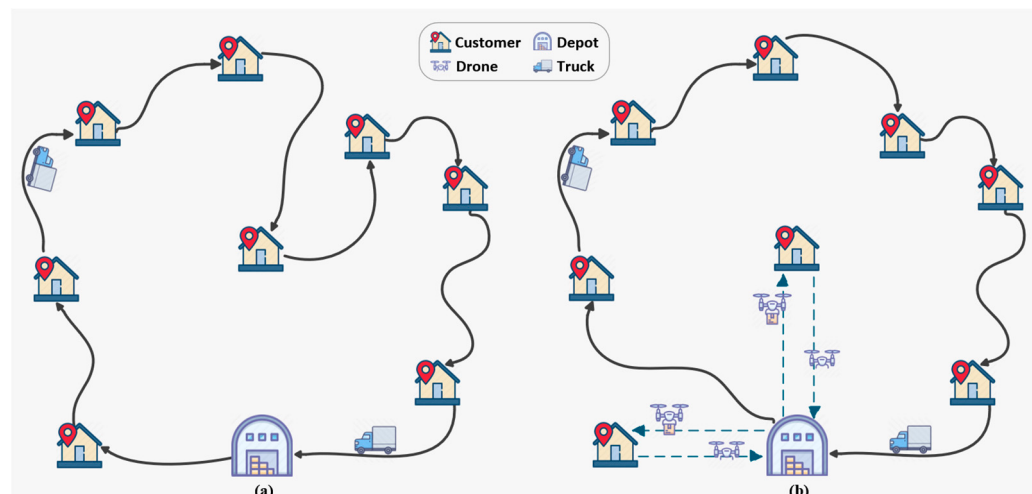


**Figure 1.** (a) Traditional delivery using only trucks; (b) Delivery with parallel system of trucks and drones.

Based on the PDSTSP proposed by [15], the model studied in this paper describes a parallel transportation operation between drones and trucks. The model can be represented as a fully directed graph  $G = \{N, A\}$ , where the set of nodes  $N = \{0, 1, \dots, n\}$  represents the depot origin (node 0) and the set of customers  $C = \{1, 2, \dots, n\}$ . The set  $A$  consists of the directed arcs between each pair of nodes. Given the load and range limitation of drones, the set of customers  $C$  is divided into two subsets: the set of customers that can only be served by ground vehicles, denoted as  $C_{gv} \subseteq C$ , and the set of “free” customers  $C_f = C \setminus C_{gv}$ , who can be served by either drones or ground vehicles. This division accounts for the fact that some customers must be served by ground vehicles due to the UAV’s load capacity, while others can be served flexibly by either UAVs or ground vehicles. Each customer’s demand is denoted by  $q_j$ , which represents the weight of the parcels to be delivered. Since last-mile transportation typically involves small to medium-sized parcels of light weight, customer demand is quantified as the weight of the corresponding parcels.

In the depot, there is a fleet consisting of  $M$  trucks and a group  $D$  of  $K$  drones, which are assigned delivery tasks. For the ground vehicles, the distance from node  $i \in N$  to node  $j \in N$  ( $j \neq i$ ) is represented as  $d_{ij}^0$ . Similarly, the flight distance for the drone from node  $i$  to node  $j$  is represented as  $d_{ij}^1$ . The travel time for the trucks on the route  $(i, j) \in A$  is represented as  $t_{ij}$ , while the total service time for the UAVs serving customers  $i \in C_f$  is represented as  $t_d$ . The service time for drones includes not only the flight time from node  $i$  to node  $j$ , but also operational time, such as loading and unloading packages. All vehicles and drones depart from the depot at the same time, starting at time  $t = 0$ ; the objective is to minimize the completion time of the entire transportation process. This completion time is defined as the time when all customers have been delivered and all vehicles and drones return to the depot. Each drone has a maximum load capacity,  $Q_d$ , set at 2.5 kg [7], ensuring it does not exceed carrying limit. During preprocessing, this constraint determines whether a customer’s demand can be handled by a drone. Only those customers whose demands do not exceed the maximum capacity are assigned to the drone for service. Similarly, trucks are constrained by their load capacity,  $Q_{gv}$ , which is set at 1300 kg, to prevent overloading during transportation. This load capacity constraint applies to the allocation of customers to the trucks as well. To more accurately reflect the actual delivery scenarios, the travel distances for vehicles are calculated using the Manhattan distance, as vehicles typically travel along the city’s orthogonal road network. For drones, the travel distances are calculated using the Euclidean distance, as drones can fly directly from one point to another without being constrained by ground traffic.

The objective of the model is to minimize the completion time of the entire transportation process. The completion time is defined as the time when all customers have been delivered, and all vehicles and drones return to the depot. The model incorporates constraints on load capacities, travel distances, and operational parameters to reflect realistic delivery scenarios. The following assumptions are established:

- (1) Customer Coverage: Not all deliveries can be accomplished by trucks or drones. Some customers can only be served by trucks, while others can be served by either drones or trucks. Each customer is served only once, ensuring that only one delivery occurs per destination;
- (2) Refueling Time for Trucks: For trucks powered by internal combustion engines, the time spent refueling during transit is not considered in the model, simplifying the operational constraints;
- (3) Time Window Constraints: Customer-specific delivery time requirements are not accounted for in the model, meaning there are no time window restrictions for deliveries;

- (4) Drone Capacity: Each drone is limited to carrying one parcel per trip. After completing a delivery, the drone must return to the depot for replenishment before commencing the next delivery task;
- (5) Annual Operation Time: Both trucks and drones are assumed to operate for 300 working days per year, with 8 h of daily operation. This results in a total annual operation time of 2400 h (8 h/day × 300 days/year);
- (6) Constant Speed: Both trucks and drones are assumed to travel at a constant speed during the entire transportation;
- (7) Hovering Time: According to [48], the hovering time of the drone is set to 30 s. This is defined as the duration the drone remains stationary in the air before descending to the customer's destination for delivery;
- (8) Legality of Operations: Both drones and trucks operate within the legal frameworks and regulations, ensuring compliance with local laws and requirements for all transportation activities.

### 3.2. Mathematical Model

This paper analyzes a transportation model, formulated as a MILP problem, involving parallel delivery operations by trucks and drones, where each customer is served exactly once. Trucks complete their delivery tasks by departing from the depot, visiting all assigned customers sequentially, and returning to the depot after finishing the assigned route. Drones, on the other hand, perform single delivery tasks by shuttling between the depot and individual customers. Due to practical constraints, such as oversized parcels, certain deliveries cannot be performed by drones. Additionally, both drones and trucks are limited by factors such as payload capacity, flight endurance, and maximum operating time. In scenarios where drones are excluded from the fleet, the transportation fleet comprises solely either fuel-based or electric trucks alone, as outlined in Section 3.1. The primary objective of this study is to minimize the total completion time for the delivery tasks. By achieving this, the model aims to enhance logistics efficiency and improve customer satisfaction. Furthermore, minimizing total completion time provides robust data for comprehensive environmental and economic assessments.

The formulation employs the following variables:

- $x_{ij}^m$ : When truck  $m$  travels from node  $i \in N$  to node  $j \in N$ , this binary variable takes the value of 1; otherwise, it takes the value of 0;
- $y_i^k$ : When node  $i \in C_f$  is visited and served by drone  $k \in D$ , this binary variable takes the value of 1; otherwise, it takes the value of 0;
- $w_i$ : A continuous variable representing the weight of the parcels carried by the truck when it reaches node  $i \in C$ ;
- $q_j$ : The demand of customer  $j$ , i.e., the weight of parcels to be delivered at node  $j \in C$ .

The model is:

**Objective:**

$$\text{Minimize } T \quad (1)$$

The objective function (1) seeks to minimize the total completion time, which is defined as the time from the start of operations until all deliveries are completed and the vehicles and drones return to the depot. This function directly captures the operational efficiency of the logistics system, promoting effective resource utilization and streamlined delivery.

The constraints of the model can be categorized into three types: completion time constraints, service constraints and variable constraints.

### Completion time constraints:

$$T \geq \sum_{(i,j) \in A} t_{ij} x_{ij}^m \quad (1 \leq m \leq M) \quad (2)$$

$$T \geq \sum_{i \in C_f} t_d y_i^k \quad (1 \leq k \leq K) \quad (3)$$

Constraints (2) and (3) establish the lower bounds on the total completion time by considering the individual completion times of each truck and drone, respectively. These constraints ensure that the total completion time is at least as long as the time required for each truck and each drone to complete their tasks.

### Service constraints:

$$\sum_{i \in C} x_{0i} \leq h \quad (4)$$

$$\sum_{\substack{i \in N \\ i \neq j}} x_{ij}^m - \sum_{\substack{i \in N \\ i \neq j}} x_{ji}^m = 0 \quad \forall j \in N \quad (5)$$

$$\sum_{\substack{i \in N \\ i \neq j}} x_{ij}^m + \sum_{k \in D} y_j^k = 1 \quad \forall j \in C_f \quad (6)$$

$$\sum_{\substack{i \in N \\ i \neq j}} x_{ij}^m = 1 \quad \forall j \in C_{gv} \quad (7)$$

$$w_i - w_j + Q_{gv} x_{ij} \leq Q_{gv} - q_j \quad (8)$$

$$\sum_{j \in C_f} y_j^k t_d \leq T' \quad \forall k \in D \quad (9)$$

$$q_j \leq Q_d \quad (10)$$

Constraints (4) to (10) ensure the feasibility, continuity, and safety of the transportation model by addressing key operational requirements. Constraint (4) limits the number of trucks departing from the depot, ensuring an efficient allocation of resources. Constraint (5) establishes a flow conservation condition for each truck, meaning that each truck must leave a customer node after completing a delivery. Constraint (6) guarantees that each customer node is visited exactly once by either a truck or a drone, avoiding duplicate visits. Constraint (7) specifies that certain customer nodes, which are restricted to truck service due to operational requirements or package characteristics, must be served by trucks. To prevent invalid routing, Constraint (8) employs the Miller–Tucker–Zemlin (MTZ) sub-tour elimination method and capacity constraints to prevent sub-tours and ensure that the truck's total load remains within its capacity [26]. Constraints (9) and (10) address UAV operations, limiting their total operating time and ensuring that the weight of parcels carried does not exceed the drones' load capacity, thereby guaranteeing safe and efficient transportation.

### Variable constraints:

$$x_{ij}^m \in \{0, 1\} \quad \forall i, j \in N, i \neq j \quad (11)$$

$$y_i^k \in \{0, 1\} \quad \forall i \in C_f, k \in D \quad (12)$$

$$0 \leq w_i \leq Q_{gv} \quad \forall i \in C \quad (13)$$

Constraints (11) to (13) define the permissible ranges for all decision variables, ensuring the solutions are feasible and valid.

## 4. Materials and Methods

This section describes a new framework for life cycle assessment (LCA) and overall life cycle cost analysis (LCCA), aimed at evaluating the environmental and economic impacts of the transportation system involving drones and trucks.

### 4.1. Life Cycle Assessment

Life Cycle Assessment (LCA), as outlined by [49], comprises four key phases: Goal and scope definition, Life cycle inventory analysis, Life cycle impact assessment and Life cycle interpretation. LCA evaluates the environmental impacts of an asset throughout its entire life cycle, encompassing raw material extraction, manufacturing, usage, and recycling or disposal. In accordance with these guidelines, this study begins by defining the scope of the life cycle, establishing the system boundary. Following this, the life cycle is divided into phases, with a detailed analysis of the inputs and outputs associated with each phase.

#### 4.1.1. Goal and Scope Definition

The scope of the Life Cycle Assessment (LCA) for this study is illustrated in Figure 2, based on the methodology described in [9]. The life cycle of the transportation system is divided into three phases: (1) the production phase, (2) the operational phase, and (3) the end-of-life (recycle) phase. In the production phase, the manufacturing processes of trucks, drones, and batteries generate emissions. During the operational phase, emissions arise from the production and supply of fuel and electricity, battery charging, and the operation of the transportation system, which can also cause noise pollution. In the end-of-life (recycle) phase, the recycling of truck bodies, drone bodies, and batteries can effectively reduce associated emissions. These unit processes are evaluated using the Global Warming Potential (GWP), quantified in terms of greenhouse gas emissions measured in kilograms of carbon dioxide equivalent (CO<sub>2</sub>e). For this analysis, the lifespan of trucks is set at 10 years, and drones at 5 years, based on [11].

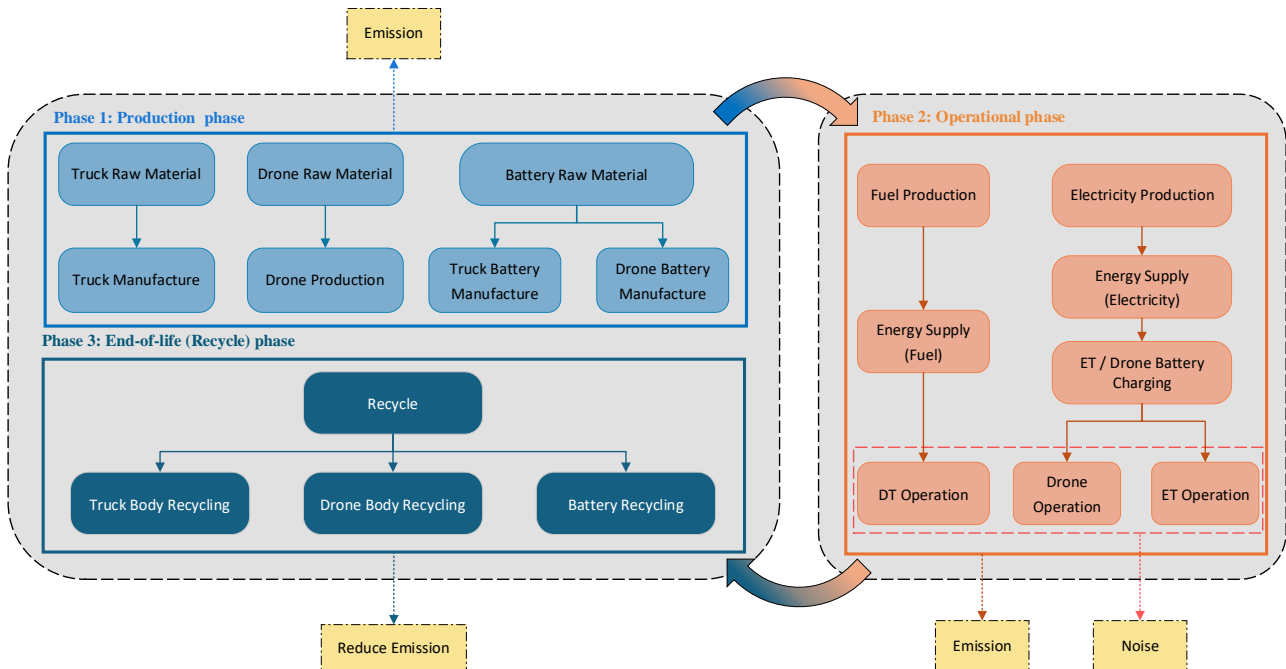


**Figure 2.** The scope of LCA.

#### 4.1.2. Production and End-of-Life Phase

The emission model for truck production has been adapted from the work of [50]. In the case of Fuel Trucks (FTs), the emissions during the production phase are estimated as follows:

$$Emission_P^{FT} = C_t \cdot W_{FT} \quad (14)$$

where  $C_t$  denotes the emission coefficient for the production of truck body parts (kg CO<sub>2</sub>e/kg) and  $W_{FT}$  is the curb weight of the FT (kg).

In the case of Electric Trucks (ETs), emissions during the production phase are more complex, as they are primarily associated with battery production [50]. Thus, the total emissions are computed from both the vehicle body production and the battery production. The emissions for ETs are given by:

$$Emission_P^{ET} = C_t \cdot W_{ET} + C_{batt} \cdot Cap_{batt} \cdot n \quad (15)$$

where  $W_{ET}$  is the curb weight of the ET (kg),  $C_{batt}$  is a constant denoting the emissions from the vehicle's battery production per unit capacity (kg CO<sub>2</sub>e/kWh),  $Cap_{batt}$  denotes the nominal battery capacity of the vehicle (kWh), and  $n$  refers to the number of batteries per vehicle.

For drones, Figllozzi [9] provides the similar expression as follows:

$$Emission_P^{drone} = C_{drone} \cdot W_{drone} + C_{batt} \cdot Cap_{batt} \cdot n \quad (16)$$

where  $C_{drone}$  is the emission coefficient for producing drone parts (kg CO<sub>2</sub>e/kg) and  $W_{drone}$  is the weight of drone without payload and battery (kg).

The end-of-life phase typically involves recycling, which can significantly reduce emissions. According to [51], savings in emissions during recycling account for approximately 17% of the emissions linked to body production.

#### 4.1.3. Operational Phase

This section describes the energy consumption and emissions of the transportation system during its operational phase. By analyzing the energy usage patterns of drones and trucks in the delivery process, this study provides a detailed assessment of their environmental impacts, enabling a more accurate quantification of their respective energy consumption levels and carbon emissions.

##### (1) Drone

To compute the total energy consumption of drones during their operational phase, this study employs the formula proposed by [52] and further refined by [7]. This formula accounts for the energy utilized across all flight phases, including takeoff, cruise, hovering, and landing, providing a comprehensive estimation of drone energy consumption.

$$P^{drone} = P^{air} + \kappa P^{lift} + P^{profile} + P^{climb} + P^{int} \quad (17)$$

$$= \frac{1}{\eta^{drone}} \left( \frac{1}{2} \rho \left( \sum_{k=1}^3 C_{D_k} A_k \right) v^3 + \kappa T w + \kappa_2 \left( g \sum_{k=1}^3 m_k \right)^{1.5} + \kappa_3 \left( g \sum_{k=1}^3 m_k \right)^{0.5} v^2 \right)$$

where  $P^{air}$  denotes the power required for the drone to overcome air resistance,  $P^{lift}$  denotes the power needed to generate lift,  $P^{profile}$  is the power required by the drone rotors to overcome air resistance,  $P^{climb}$  is the power needed for climbing, and  $P^{int}$  denotes the power consumed by internal electronic components. Definitions of other parameters are provided in Tables 1 and 2.

In UAV energy consumption modeling, a flight is typically divided into four phases: (i) takeoff, (ii) level flight, (iii) hovering, and (iv) landing. Figure 3 illustrates the UAV flight patterns during an ideal operational phase [48]. Based on these patterns, the total energy consumption for UAV transportation in an ideal scenario can be expressed as follows:

$$E^{drone} = \frac{1}{\eta_c^{drone}} \left( t_{tol} \left( P^{drone}(m, v, 45^\circ) + P^{drone}(m, v, -45^\circ) \right) + t_{lf} P^{drone}(m, v, 0^\circ) + t_{hover} P^{drone}(m, |v_{head}|, 0^\circ) \right) + t P^{int} \quad (18)$$

where  $t_{tol}$  denotes the time consumed during takeoff and landing,  $t_{lf}$  denotes the cruising time,  $v_{head}$  is the headwind velocity, and  $t$  is the total flight time. All flight phases are taken into account, with both ascent and descent angles set at  $45^\circ$ . Weight is a relevant variable in the delivery process, as it directly influences the power consumption of the drone. According to the formula, the total mass during the delivery phase is represented as  $m = \sum_{k=1}^3 m_k$ , which includes the payload. During the return-to-depot phase, the mass is adjusted to  $m = \sum_{k=1}^3 m_k - m_3$ , as the payload is no longer carried on the return trip after delivery. Since the maximum weight that the drone can carry is set at 2.5 kg, payloads below this weight have a relatively minor impact on the drone's autonomy and do not significantly affect its overall performance [7]. The cruising altitude is set to 120 m. Assuming the drone maintains a constant speed across all flight phases, with takeoff and landing speeds being lower than the cruise speed, the cruise speed is set at 17 m/s, while the average takeoff/landing speed is 2.3 m/s. Detailed formulas and other relevant UAV specifications can be found in Tables 1 and 2 [7,11,53].

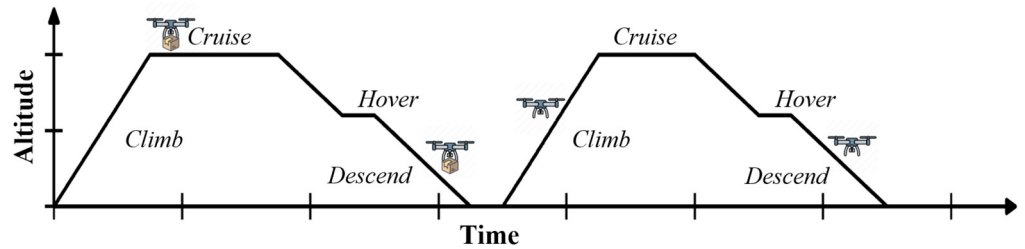


**Figure 3.** UAV delivery flight pattern.

**Table 1.** Formulas for drone energy consumption model.

Description	Formula
Thrust	$T = \sqrt{\left(g \sum_{k=1}^3 m_k\right)^2 + \left(\frac{1}{2}\rho \left(\sum_{k=1}^3 C_{Dk} A_k\right) v^2\right)^2} + \rho \left(\sum_{k=1}^3 C_{Dk} A_k\right) v^2 m_1 g \sin \theta$
Downwash coefficient	$w$ can be found by solving the following equation $w = \frac{T}{2\rho r^2 \pi n_{rotors} \sqrt{(v \cos \alpha)^2 + (w - v \sin \alpha)^2}}$ $\alpha = \tan^{-1} \left( \frac{\frac{1}{2}\rho \left(\sum_{k=1}^3 C_{Dk} A_k\right) v^2}{g \sum_{k=1}^3 m_k} \right)$
Angle of attack	
Time for takeoff and landing	$t_{tol} = \frac{a}{\sin 45^\circ v_{lf} - v_{wind}}$
Time for level flight	$t_{lf} = \frac{d_{drone}}{v_{lf} - v_{wind}} - 2t_{tol}$
Total time for the entire flight phase	$t = t_{lf} + t_{hover} + 2t_{tol}$

**Table 2.** Input values for drone energy consumption model.

Abbreviation	Description	Unit of Measure	Value
$\rho$	Air density	(kg/m <sup>3</sup> )	1.225
$g$	Acceleration of gravity	(m/s <sup>2</sup> )	9.807
$v$	Flight speed	(m/s)	/
$v_{level}$	Flight speed during level flight	(m/s)	17
$v_{tl}$	Flight speed during taking off and landing	(m/s)	2.3
$k$	Drone body = 1; Drone battery = 2; Payload (package) = 3		/
$C_{drone}$	Emission coefficient for drone	(kg CO <sub>2</sub> e/kg)	9.3
$W_{drone}/m_1$	Mass of drone body	(kg)	8
$C_{batt}$	Emission coefficient for battery	(kg CO <sub>2</sub> e/kWh)	141
$Cap_{batt\ drone}$	Nominal drone battery capacity	(kWh)	0.8
$m_2$	Mass of drone battery	(kg)	6.15
$C_{D_1}$	Drag coefficient of drone body		1.49
$C_{D_2}$	Drag coefficient of drone battery		1
$C_{D_3}$	Drag coefficient of payload		2.2
$A_1$	Surface area of drone body	(m <sup>2</sup> )	0.224
$A_2$	Surface area of drone battery	(m <sup>2</sup> )	0.015
$A_3$	Surface area of payload	(m <sup>2</sup> )	0.0929
$\kappa$	Factor for induced power		1.15
$\kappa_2$	Factor for profile power	((m/kg) <sup>1/2</sup> )	0.68
$\kappa_3$	Factor for profile power associated with speed	((m/kg) <sup>1/2</sup> )	0.087
$P_{avio}$	Power required for all avionics on the drone	(Watt = J/s)	30
$\eta^{drone}$	Battery and motor power transfer efficiency		0.9
$\eta_c^{drone}$	Battery charging efficiency		0.9
$\theta$	Flight angle (i.e., $\theta = 0$ for level flight)		Discussed in the text
$r$	Rotor radius	(m)	0.4
$n_{rotors}$	Number of rotors		8
$a$	Level flight altitude	(m)	120
$d_{drone}$	Distance during level flight	(m)	Discussed in the text
$f_{kwh}$	The coefficient from kJ to kWh	(kJ/kWh)	0.0002778

## (2) Ground vehicles

Similarly, the energy consumption of ground vehicles during operation can be divided into the following four components, based on [7]:

$$P^{GV} = P^{roll} + P^{air} + P^{grade} + P^{inert} \quad (19)$$

$$= c_{roll} m_G g v_G + \frac{\rho c_{air}}{2000} A_G v_G^3 + i m_G g v_G + \frac{0.54 n^{acc}}{7200} m_G (v_G * 3.6)^3$$

where  $P^{roll}$  denotes the power required to overcome rolling resistance;  $P^{air}$  denotes the power required to overcome air resistance;  $P^{grade}$  represents the power required to overcome gravitational forces; and  $P^{inert}$  is the power required for internal mechanical consumption.

Due to differences in energy sources, FTs operate using diesel engines, while ETs utilize electric motors. As a result, their energy consumption models differ in structure and calculation. The energy consumption model for fuel trucks is expressed as:

$$F^{DT}(d_{GV}, v_G, n^{acc}) = \frac{d_{GV}}{v_G} \left( f^{idle} + \frac{f^{full} - f^{idle}}{P\eta^{DT}} P^{GV}(d_{GV}, v_G, n^{acc}) \right) \quad (20)$$

where  $f^{idle}$  and  $f^{full}$  denote the fuel consumption rates (in liters per hour) during idle and full-throttle modes, respectively, while  $P$  denotes the engine power. The conversion efficiency of the diesel engine,  $\eta^{DT}$ , is typically calculated using the following formula:

$$\eta^{DT} = 0.90 - 0.72e^{-0.077v_G^{1.41}} \quad (21)$$

For ETs, the total energy consumption during operation is modeled as follows:

$$E^{ET}(d_{GV}, v_G, n^{acc}) = \frac{d_{GV} P^{GV}(d, v_G, n^{acc})}{v_G \eta^{ET}}. \quad (22)$$

where  $\eta^{ET}$  denotes the total tank-to-wheels (TTW) energy efficiency of the electric truck, which can be calculated using the following formula:

$$\eta^{ET} = \eta_e^{ET} \eta_t^{ET} \eta_c^{ET} \quad (23)$$

As with drones, the mass  $m_G$  of trucks changes as deliveries are completed, with the payload reduced after each delivery. During the return phase, the truck operates without payload, assuming all assigned deliveries are completed. The maximum payload capacity of each truck is set at 1300 kg. Detailed truck-related specifications and parameters are provided in Table 3, referencing [7,53].

**Table 3.** Input values for ground vehicles energy consumption model.

Abbreviation	Description	Unit of Measure	Value
$A_G$	Frontal surface area of ground vehicles	(m <sup>2</sup> )	6
$C_t$	Emission coefficient for truck	(kg CO <sub>2</sub> e/kg)	8
$Cap_{batt\ et}$	Usable truck battery capacity	(kWh)	105
$c_{roll}$	Rolling resistance coefficient		0.008
$c_{air}$	Aerodynamical drag coefficient		0.65
$W_{DT}$	Mass of FT	(kg)	2670
$W_{ET}$	Mass of ET	(kg)	2940
$v_G$	Speed of ground vehicles	(m/s)	Discussed in the text
$i$	Road grade		0.9995
$d_{GV}$	Distance covered by ground vehicles	(m)	Discussed in the text
$n^{acc}$	Acceleration frequency coefficient		Discussed in the text
$P$	Engine Power	(kW)	150
$f^{idle}$	Fuel consumption rates in idle mode	(l/h)	1
$f^{full}$	Fuel consumption rates in full-throttle mode	(l/h)	25
$\eta^{DT}$	Transmission efficiency of fuel trucks		0.9
$\eta^{ET}$	Total TTW efficiency of electric trucks		0.729
$\eta_e^{ET}$	Engine efficiency of electric trucks		0.9
$\eta_t^{ET}$	Transmission efficiency of electric trucks		0.9
$\eta_c^{ET}$	Battery charging efficiency of electric trucks		0.9

To calculate emissions during the operational phase, ref. [13] provides the following equation:

$$Emission_O = ef_{kwh}E \quad (24)$$

where  $e$  represents the amount of carbon dioxide ( $\text{CO}_2$ ) emitted per unit of energy consumed (in  $\text{kg-CO}_2/\text{kWh}$ ),  $f_{kwh}$  is the conversion coefficient from  $\text{kJ}$  to  $\text{kWh}$ , and  $E$  denotes the energy consumption of the transportation vehicle.

For fuel vehicles, emissions are based on the total well-to-wheel (WTW) emissions, which are the sum of the well-to-tank (WTT) emissions and TTW emissions. The WTT emissions are related to the extraction, transportation, and refining of diesel fuel, while the TTW emissions are generated by the combustion of the diesel fuel in the truck's internal combustion engine. To calculate the total WTW emissions, the emission factor for diesel fuel is used, which is 3.24 kg  $\text{CO}_2$  per liter of fuel [7].

$$Emission_{DT} = WTW \cdot F^{DT}(d_{GV}, v_G, n^{acc}) \quad (25)$$

The total life-cycle emissions include emissions from the production phase, the operational phase, and the savings from the recycling phase:

$$Emission_{total} = Emission_P + Emission_O - Emission_{saving} \quad (26)$$

#### 4.1.4. Noise Model

Quantifying the noise levels during both the production and end-of-life phases is challenging, making the operational phase the primary focus for noise evaluation.

In the evaluation of vehicular noise, we have adopted models presented by [41]. To compute the noise contribution of the vehicle  $i$  (dB) at a given location  $S_m = (a_m, b_m, c_m)$ , the expression is as follows:

$$L_i(S_m) = L_1 - \left| 10 \log_{10} \left( S_m - S_i^2 \right) \right| \quad (27)$$

where  $S_i = (a_i, b_i, c_i)$  is the location of the vehicle. For fuel trucks, the noise level is set at 80 dB, while for electric trucks, it is 70 dB, and for drones, it is 90 dB.

Then, under the assumption that the noise level follows a logarithmic model during parallel delivery by a drone and trucks, the noise level at location  $S_m$  is determined by their combined influence. And the model is expressed as follows:

$$L(S_m) = 10 \log_{10} \left( \sum_{i=1}^2 10^{\frac{L_i(S_m)}{10}} \right) \quad (28)$$

To simplify the noise modeling process, the city is modeled as an open field without obstructions, excluding sound reflections or barriers. This abstraction is used to isolate the combined noise impact without incorporating the complexities of urban sound dynamics, such as reflections and diffractions specific to the urban environment.

#### 4.2. Life Cycle Cost Analysis

To investigate and compare the life-cycle economics of ground vehicles and drones, this study draws on the Life-cycle Cost Analysis (LCCA) framework proposed by [54,55]. To account for UAV-related environmental costs and additional operational expenses, the analysis includes emissions and carbon market fees. As Figure 4 shows, the entire economic life cycle is divided into the following phases: (1) Initial Cost, which includes equipment procurement and setup costs; (2) Energy Cost, covering the energy required during operation; (3) Environmental Costs, which account for the costs associated with

carbon emissions; (4) Operating Costs, which encompass expenses for daily operations and maintenance, such as repairs; and (5) Residual Value, referring to the equipment's value at the end of its useful life. It is important to note that some cost factors (such as taxes, insurance, and fines) are excluded from this study due to their high uncertainty and difficulty in accurate estimation.

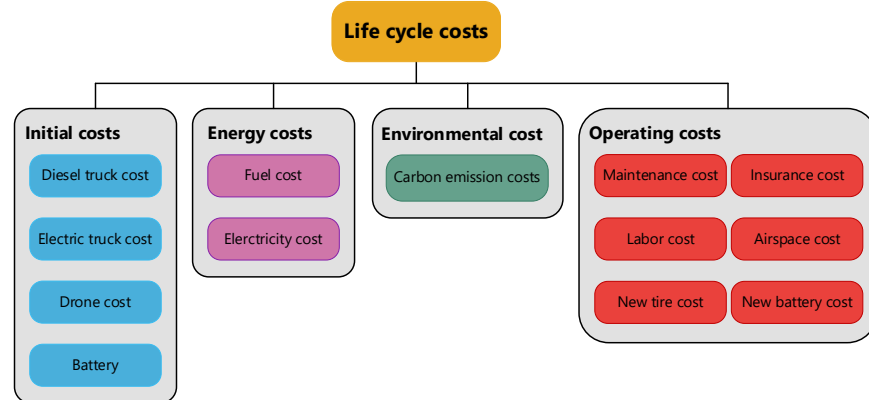


**Figure 4.** The scope of LCCA.

In the cost calculation, this study employs the Net Present Value (NPV) method to enable a clear comparison and accurate calculation of all relevant costs. The rationale for selecting the NPV method is its ability to convert future cash flows into present values, thereby providing a consistent approach to assess costs and benefits at different time points. This method is particularly appropriate for life cycle analysis, as it incorporates the time value of money, allowing for a direct comparison of costs and benefits incurred at various stages throughout the life cycle.

To calculate the NPV, we converted all future cash flows to present value using 2024 as the base year. The specific calculation formula is shown below:

$$PV = \frac{FV}{(1+r)^y} \quad (29)$$

where  $FV$  represents the future value,  $r$  is the discount rate, and  $y$  is the time period, which in this study refers to the number of years in the life cycle.

Table 4 presents the values of all the parameters discussed, with primary references to [11,13,56]. All currency values have been converted to CNY (Yuan). The discount rate  $r$  is set at 10%.

**Table 4.** Summary of all the cost parameters used in the economic assessment.

Parameter	Unit of Measure	Value
Fuel truck cost	CNY	361,003
Electric truck cost	CNY	469,200
Drone cost	CNY	156,400
Drone battery cost	CNY	500
Truck battery cost	CNY	85,342
Cost of new battery	CNY/kWh	510
Unit carbon-emission cost	CNY/kg-CO <sub>2</sub>	0.030
Fuel truck maintenance cost	CNY/km	0.321
Electric truck maintenance cost	CNY/km	0.163
Drone maintenance cost	CNY/year	13,300
Truck insurance cost	CNY/year	4692
Drone insurance cost	CNY/year	7820
Airspace cost	CNY/h	15
Cost of new tire	CNY/km	0.352

#### 4.2.1. Initial Costs

Initial Costs generally encompass a range of expenditures, such as procurement, construction, and refurbishment. However, for the purposes of this study, which emphasizes a life cycle analysis focused on transportation, initial costs refer specifically to the expenditures associated with the purchase of transportation equipment and its accessories. This includes the acquisition cost of fuel vehicles, electric trucks, drones, and batteries.

#### 4.2.2. Energy Costs

Energy costs, in the context of this study, refer to expenditures related to energy consumption during the operational phase. A focused consideration of energy expenditures allows better management of the associated costs while also reflecting environmental impacts. Specifically, Energy Costs in this study include the following aspects:

- (1) Fuel costs: Fuel costs primarily account for the refueling of fuel vehicles. The total annual fuel cost is determined by multiplying the unit price of fuel by the average daily kilometers and the number of working days in a year, as expressed in the following Formula (31):

$$\begin{aligned} \text{Yearly fuel cost} \\ = \text{fuel cost per kms} \cdot \text{daily kms} \\ \cdot \text{number of workdays per year} \end{aligned} \quad (30)$$

- (2) Electricity costs: Electricity costs primarily account for the expenditure on charging the batteries of electric trucks and drones during their operational phase. The total annual electricity cost is calculated by multiplying the unit price of electricity by the average daily electricity consumption (in kWh) and the number of working days in a year. This relationship is expressed as:

$$\begin{aligned} \text{Yearly electricity cost} \\ = \text{electricity cost per kWh} \cdot \text{daily kWh} \\ \cdot \text{number of workdays per year} \end{aligned} \quad (31)$$

#### 4.2.3. Environmental Cost

Environmental costs mainly refer to the financial burdens arising from the environmental impacts caused by the operation of vehicles and drones. In this study, environmental costs are primarily quantified through carbon emission fees, which are imposed by governments to regulate emissions. The carbon emission cost of ground vehicles and drones is calculated using the following equation:

$$\text{Environment responsibility cost} = C_{carbon} \cdot \text{Emission} \quad (32)$$

where  $C_{carbon}$  represents the unit price of carbon emissions. This cost not only provides an economic measure of the environmental impact of different transportation modes but also facilitates a more comprehensive evaluation of their economic feasibility and environmental benefits.

#### 4.2.4. Operating Costs

Operating Costs encompass various non-energy related costs that are necessary to maintain the regular operation of the transportation system. Operating Costs in this study include the following:

- (1) Maintenance Costs: These are the expenses incurred for the repair and upkeep of vehicles and drones to ensure their proper functioning;

- (2) Insurance Costs: This category includes the costs associated with insuring the means of transportation and their operators;
- (3) Labor Costs: Labor costs mainly include the wages of truck drivers and UAV operators, reflecting the human resource expenditures associated with operation;
- (4) Airspace cost: Although no formal charging system has been established for airspace usage, it is essential to account for airspace usage costs to ensure the financial sustainability of the UAV Traffic Management (UTM) system, mitigate air traffic congestion, and effectively manage UAV density. The airspace cost calculation method, adapted from [45], is given as follows:

$$\begin{aligned} \text{Yearly airspace cost} \\ = \text{hourly airspace cost} \\ \cdot \text{number of working hours per year} \end{aligned} \quad (33)$$

- (5) Tire replacement costs: The cost of replacing tires on ground vehicles needs to be taken into account, given that tires wear out over time and incur repair or replacement costs;
- (6) Battery replacement costs: Considering that the batteries of drones and electric trucks wear out over time, the cost of battery replacement needs to be included in the calculation.

#### 4.2.5. Residual Value

Residual value refers to the remaining worth of an asset at the end of its useful life, which can be determined based on factors such as existing value, resale value, salvage value, or scrap value, minus any related selling, conversion, or disposal costs [54]. In this study, the residual value pertains to vehicles, drones, batteries, and other components. As materials such as the vehicle body and batteries are recyclable at the end of their life cycle, certain components may be resold as spare parts. According to [50], the recycling rate for truck bodies and batteries is typically estimated at 5% of the initial cost.

## 5. An Algorithm for PDSTSP

Adaptive Large Neighborhood Search (ALNS) is a popular heuristic used to solve the Vehicle Routing Problem (VRP) and the Electric Vehicle Routing Problem (EVRP) [57]. Its basic concept revolves around iteratively improving an initial solution by applying a set of destruction and repair operators. These operators are chosen probabilistically from a predefined pool based on their historical performance. Once a new solution is generated within the neighborhood, its feasibility and quality are evaluated according to the objective function and an acceptance criterion, with feedback provided to the operators in the form of cumulative scores to guide future selections.

However, applying the traditional ALNS algorithm to the parallel transportation system in this study presents several unique challenges. These challenges arise mainly from the significant differences between drones and trucks in terms of capacity, routing, and delivery constraints. For instance, drones are typically constrained by smaller payload capacities and shorter flight ranges, while trucks can handle larger volumes and follow more intricate routing patterns. These fundamental differences necessitate a joint consideration of both transport modes during operator selection and solution evaluation. This added layer of complexity increases the difficulty of designing appropriate operators and accurately assessing solution feasibility and performance.

To adapt the traditional ALNS algorithm to the parallel truck-and-drone transportation system, two key improvements are introduced. First, to address the allocation of customer points between trucks and drones, a variant of the Best Insertion heuristic and a new greedy strategy, Greedy Truck-First, Drone-Second, are incorporated. This strategy prioritizes trucks for initial allocations and then assigns tasks to drones based on their capacities

and ranges, optimizing the allocation process and improving solution quality. Second, to overcome the tendency of the traditional ALNS algorithm to get trapped in local optima, the Simulated Annealing (SA) criterion is employed as the solution acceptance rule. By allowing the occasional acceptance of worse solutions with a probability, this approach broadens the search space and increases the likelihood of finding globally optimized solutions. Together, these enhancements improve allocation efficiency, expand the solution search range, and enhance overall optimization in the parallel transportation system [58].

Considering these improvements, the workflow of the ALNS algorithm includes the following steps: It begins with an initial solution. Adaptive destruction and repair operators are then selected from this solution to generate the neighborhood. The SA criterion is subsequently applied to assess the quality of the candidate solutions. Moreover, both the selection probabilities of the operators and the acceptance probability are dynamically adjusted throughout the process. This iterative procedure continues until the termination conditions are satisfied, at which point the algorithm outputs the optimal solution, as illustrated in the algorithm flow shown in Figure 5.

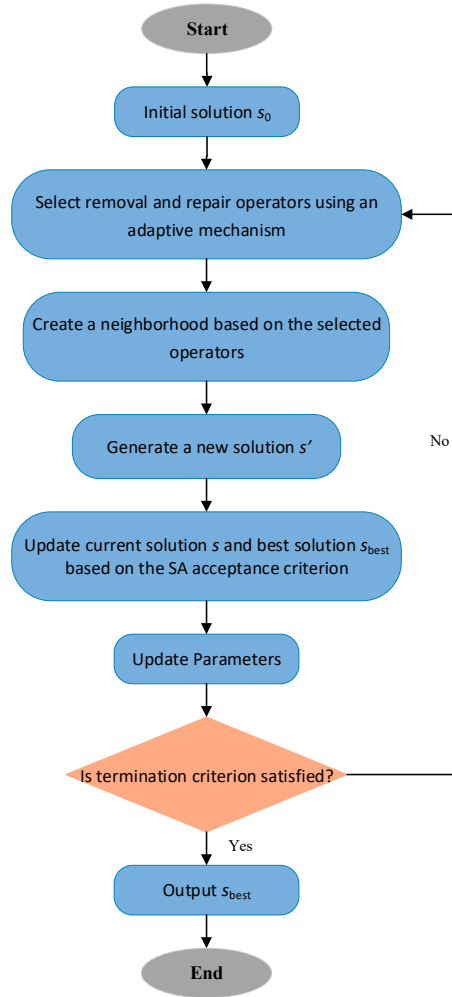


**Figure 5.** An illustration of the general framework of the ALNS algorithm.

### 5.1. Initial Solution Generation

The initial solution is generated using a greedy insertion method that involves two main steps. First, in Step 1, the customer node with the highest demand is selected to be served by the trucks in the route, and customers are considered to be inserted in descending order of demand. Then, Step 2 calculates the insertion completion time for each unassigned customer by comparing two cost metrics: the truck's cost for traveling from the last inserted

point to the uninherited customer and the drone's cost for serving the uninherited customer directly from the depot. The option with the smallest completion cost is chosen, and the corresponding insertion operation is performed. During this step, both truck and drone service options are evaluated for each customer, ensuring that a feasible route is maintained (with the fallback of assigning a new truck for individual customer service if required). Step 2 is repeated iteratively until all customers are successfully inserted into feasible routes.

### 5.2. Destroy Operator and Repair Operator

The solution is improved through destroy and repair processes, which involve determining the number of nodes to be removed and reinserting them into the solution. Initially, a predefined number of nodes are selected for removal, and an empty removal set is created. The removal operator is then applied to select customers and transfer them into the removal set. Next, the insertion operator reinserts all removed customers back into the partially destroyed solution, one by one, until the removal set is empty. This iterative destroy and repair process creates new neighborhoods, promoting solution diversity.

To enhance the algorithm's flexibility and adaptability, five deletion operators and five insertion operators are introduced, which offer diverse strategies for manipulating the solution during the neighborhood generation phase. These operators collectively ensure a broader exploration of the solution space while maintaining feasibility.

#### 5.2.1. Destroy Operator

Traditional destroy operators often focus on simple strategies like random or systematic node removal, but these methods can lead to local optimality. To address this limitation, the destroy operators for the model in this study incorporate more sophisticated strategies to explore the solution space efficiently, prevent local optimality, and better meet the model's requirements.

- (1) Random removal: This strategy involves randomly selecting and removing a specified percentage of nodes from the current solution. By quickly altering the solution's structure, this method reduces the likelihood of the algorithm becoming trapped in a local optimum;
- (2) Cluster removal: This operator starts by randomly selecting a customer point to define the centroid for removal. The initially chosen customer and nearby customers, determined based on proximity to the centroid, are removed iteratively until a predefined removal count ( $\beta$ ) is reached. At each iteration, the next node to be removed is randomly selected from the two closest neighbors to the centroid. By focusing on a localized region while introducing randomness, this method avoids producing repetitive partial solutions and fosters a global search direction. The corresponding pseudo-code is provided in Algorithm 1;
- (3) Worst removal: This operator targets the removal of customer points that contribute the most to the objective function value, specifically those with the greatest impact on minimizing the completion time. All vertices are iterated through and sorted in ascending order based on the magnitude of the change in the objective value resulting from their removal. By systematically eliminating the customer points with the largest negative impact on the current solution's objective value, this method enhances the algorithm's efficiency and guides the search towards improved solutions;
- (4) Shaw Removal [59]: The Shaw removal operator is designed to enhance the destructiveness of the solution by removing customers that are similar to the starting node. This helps the algorithm escape local optima and perform a more extensive search. The process begins by defining a removal ratio, which typically ranges between a minimum and maximum threshold. Next, the correlation score between each remaining

customer node and the starting node is calculated, based on two factors: the demand difference and the distance between the customer and the starting node. The node with the smallest correlation score is selected for removal. This process is repeated until the predetermined number of nodes is removed. The formula for calculating the correlation score is as follows:

$$R(i, j) = \chi_d d_{ij} + \chi_q |q_i - q_j| \quad (34)$$

where  $d_{ij}$  represent the distance between customer  $i$  and  $j$ , while  $q_i$  and  $q_j$  denote the demands of customer  $i$  and  $j$ , respectively.  $\chi_d$  and  $\chi_q$  are the operator parameters used for normalization. The smaller correlation score  $R(i, j)$  means higher relatedness between customers;

- (5) Worst drone removal: This operator is similar to the traditional worst removal operator but specifically targets the removal of drone paths that contribute the most to the objective function, thereby improving the overall efficiency of the algorithm.

---

**Algorithm 1:** Cluster Removal
 

---

**Input:** Current solution:  $s$ ,  
Number of customers to remove:  $\beta$   
**Output:** Updated list of removed customers:  $remove\_list$

```

1  total_nodes ← Number of customer nodes in  $s$ 
2  if total_nodes ≤  $\beta$  then
3    return All node indices from 0 to  $total\_nodes - 1$ 
4  end if
5  remove_list ← []
6  center_idx ← Randomly select an index from 0 to  $total\_nodes - 1$ 
7  remove_list.append (center_idx)
8  distances ← distances from the center node to all other nodes
9  distances.sort()
10 for  $i \leftarrow 0$  to  $\beta - 1$  do
11   remove_list.append (distances[i].index)
12 end for
13 return remove_list

```

---

### 5.2.2. Repair Operator

Traditional repair operators typically reinsert unassigned nodes into existing routes through a simple insertion operation. However, these approaches may not fully take into account the complexity of multiple service modes (drones and trucks). Therefore, for the parallel drone and truck transportation model in this paper, we introduce the following more complicated strategy in designing the repair operator, aiming to adapt more precisely to the model requirements and improve the overall efficiency and optimization capability of the algorithm.

- (1) Best insertion [60]: This operator is designed to optimize the reinsertion of deleted customers into existing routes or create new routes, considering both trucks and drones simultaneously. The strategy includes three variants to improve flexibility and efficiency: The first variant randomly selects a customer from the removal set and inserts it into the location that incurs the least additional time or cost, promoting diversity in the solution and helping avoid local optima. The second variant prioritizes customers who have not yet been served by drones, thereby freeing up more insertion locations for other customers that might be better served by trucks. This is particularly useful in situations where drones have limited capacity or when they are more efficient

for small, high-density areas. The third variant directly selects customers who have been served by drones, ensuring all customers are assigned to a transportation mode. Each variant is weighted by the coefficients  $g_1$ ,  $g_2$ , and  $g_3$  ( $g_1 + g_2 + g_3 = 1$ ) and selected probabilistically using the roulette wheel mechanism. The corresponding pseudo-code is shown in Algorithm 2;

---

**Algorithm 2:** Best Insertion
 

---

**Input:** Remove nodes:  $remove\_list$ ,  
Customer Sets:  $C_{gv}$ ,  $C_f$   
**Output:** New solution:  $s'$

```

1 Initialize unassigned_nodes, assigned_nodes
2 for each customer node do
3   if customer node in remove_list then
4     Add to unassigned_nodes;
5   else
6     Add to assigned_nodes
7   end if
8 end for
9 Classify unassigned_nodes into  $C_{gv}$  and  $C_f$ 
10 while unassigned_nodes not empty do
11   node  $\leftarrow$  pop from unassigned_nodes
12   rand  $\leftarrow$  random number
13   if rand  $< g_1$  then
14     Insert node at best position in assigned_nodes;
15   else if rand  $< g_1 + g_2$  then
16     Insert all from  $C_{gv}$  and  $C_f$ ;
17   else
18     For each node in  $C_f$ : Insert at best position;
19   end if
20 end while
21 return  $s'$ 
```

---

- (2) Greedy truck-first drone-second insertion: This operator aims to optimize the reinsertion of unassigned customer points. For each unassigned customer node, the algorithm calculates the expected increment in the completion time objective function for each possible insertion position, considering the customer's characteristics and transportation mode. In the first phase, if the selected customer point belongs to the ground vehicle-only set  $C_{gv}$ , the algorithm only calculates the increment when inserting the customer into the truck route. If the customer node belongs to the  $C_f$  set, which represents customers that can be served by either drones or ground vehicles, the algorithm calculates the increment for both possible assignments—one to the truck route and one to the drone route. The algorithm then compares the expected increment in completion time for both options and selects the one with the smallest increment. The corresponding pseudo-code is shown in Algorithm 3;
- (3) Greedy insertion: This operator minimizes the total cost by iteratively inserting unallocated customer nodes into the most optimal positions within existing routes. The algorithm follows a step-by-step approach, where each unallocated node is considered for insertion into every possible position within the already allocated nodes. In each iteration, the algorithm calculates the objective total completion time for every possible insertion of the unallocated node into each position in the list of already allocated nodes. After evaluating all possible positions, the node is inserted into the position that results in the lowest objective function value. Once the optimal

insertion position is found, the unallocated node is added to the route, and it is removed from the unallocated node list. This process is repeated until all customer nodes are successfully assigned to the routes, ensuring that the solution is optimized at each step;

---

**Algorithm 3:** Greedy Truck-First Drone-Second Insertion
 

---

**Input:** Remove nodes:  $remove\_list$ ,  
 Customer Sets:  $C_{gv}, C_f$   
**Output:** New solution:  $s'$

```

1 Initialize unassigned_nodes, assigned_nodes
2 for each customer node do
3   if customer node in remove_list then
4     Add to unassigned_nodes;
5   else
6     Add to assigned_nodes
7   end if
8 end for
9 while unassigned_nodes not empty do
10   node  $\leftarrow$  pop from unassigned_nodes
11   best_mode  $\leftarrow$  None
12   if node in  $C_{gv}$  then
13     Find best insertion in assigned_nodes,
14     best_mode  $\leftarrow$  truck;
15   else
16     Find best insertion in both truck and drone paths;
17     if best insertion in truck paths then
18       best_mode  $\leftarrow$  truck;
19     else
20       best_mode  $\leftarrow$  drone;
21     end if
22   end if
23   Insert node based on best_mode
24 end while
25 return  $s'$ 

```

---

- (4) Regret insertion: This operator enhances the total completion time optimization by calculating the “regret value” for each unallocated node at all possible insertion positions. The process begins by iterating through all the unassigned nodes and attempting to insert each one into every possible position in the list of already assigned nodes. For each possible insertion, the objective function value is calculated. The “regret value” is then determined for each insertion, which represents the difference between the current position’s objective function value and the best possible value that could have been achieved at that moment. Once the optimal position is found, the unassigned node is inserted into that position, and it is removed from the unallocated node list. This process is repeated until all customer nodes are successfully assigned to routes. By considering the regret value at each step, the Regret Insertion operator strategically minimizes potential incremental costs, resulting in a more optimized solution with lower total costs;
- (5) Random repair: This operator aims to quickly reconfigure the solution by inserting unassigned nodes into randomly selected positions within the already assigned nodes. This strategy involves selecting insertion locations at random, rather than following a specific optimization criterion. Once a random position is selected for each unassigned

node, it is inserted into the route, and the objective function is recalculated based on the updated solution.

### 5.3. Acceptance Criterion

The acceptance criterion determines which newly generated solutions proceed to the next iteration. If the algorithm only seeks better solutions, it may become trapped in a local optimum. Therefore, accepting inferior solutions with a certain probability helps the algorithm escape local optima and move towards a global optimum. In the SA algorithm, the acceptance criterion is as follows: when the new solution is better than the current solution, it is always accepted; when the new solution is not better, the simulated annealing mechanism is used to determine whether the solution should be accepted. The acceptance probability  $P$  is calculated as follows:

$$P = \begin{cases} 1, & f_{obj}(S') < f_{obj}(S) \\ e^{-\frac{|f_{obj}(S') - f_{obj}(S)|}{T}}, & f_{obj}(S') \geq f_{obj}(S) \end{cases} \quad (35)$$

where  $f_{obj}(S)$  represents the objective function of the current solution, and  $f_{obj}(S')$  is the objective function of the new solution.  $T$  denotes the current temperature, which is updated at each iteration according to the formula  $T = T \cdot c$ , where  $c$  is the simulated annealing parameter. As the iterations proceed, the temperature  $T$  gradually decreases. The algorithm stops when the temperature reaches a predefined threshold or when the maximum number of iterations is reached.

## 6. Results

This section presents the experimental design and the feasibility analysis of the proposed model. First, the experimental scenarios are defined, including customer distribution and parameter settings, to ensure the realism and reliability of the experiments. Second, the optimization process of the algorithm is described in detail, and the performance of the improved Adaptive Large Neighborhood Search (ALNS) algorithm is compared with that of the traditional and exact algorithms. Finally, the environmental and economic impacts under different fleet compositions are analyzed, focusing on three key metrics: carbon emissions, noise pollution, and lifecycle costs. Sensitivity analyses are conducted to explore the specific effects of three key parameters as well as two different environmental and cost scenarios on these metrics, particularly carbon emissions and transportation costs.

### 6.1. Experiment Design

#### 6.1.1. Scene Definition

Due to the limited availability of benchmark instances of transportation models similar to the one presented in this paper, this paper selects randomly generated instances for experimental testing. To ensure the practical relevance and reliability of the experimental results, the Pudong district of Shanghai is selected as the simulation test area. This region is chosen for several reasons. First, Pudong features a complex urban layout characterized by dense buildings, intricate street patterns, and an irregular road network, creating a realistic and challenging environment for simulation. Second, the region exhibits diverse traffic conditions, including congested roads in the urban core and smoother traffic flows in suburban areas. This variety provides a robust foundation for evaluating logistics and distribution scenarios under different operational conditions.

Empirical studies suggest that typical urban parcel delivery services involve approximately 100–200 customers [7]. In this study, the number of customers is set to  $n = 100$ , representing a problem scale that adequately captures the challenges of real-world trans-

portation processes. To simulate diverse delivery scenarios, this paper draws on the methodologies of [61,62] and adopts three distinct customer distribution patterns: random distribution (r), clustered distribution (c), and random-clustered distribution (rc). The random distribution models the randomness of customer locations, reflecting scenarios where delivery points are scattered across a region without discernible patterns. The clustered distribution captures the scenario where customers are concentrated in specific areas, often resembling high-density zones within urban settings. Lastly, the random-clustered distribution combines elements of both randomness and clustering, providing a more realistic representation of customer distribution complexities typical of urban environments.

### 6.1.2. Scenario Setup

#### (1) Fleet combinations

We set up four fleet combinations to evaluate operational efficiency and cost across different configurations: 1 drone + 1 EV, 2 drones + 1 EV, 2 EVs, and 2 FTs. Detailed specifications of each configuration are provided in Table 5. The primary aim of analyzing these combinations is to uncover variations in delivery efficiency, cost, and environmental impact. By comparing these setups, we aim to assess the performance differences across diverse fleet combinations. The configurations for each fleet combination are presented in Table 5. The combination of 1 drone + 1 EV, referred to as DT1, serves as the baseline mixed delivery mode, designed to evaluate performance under standard conditions. The setup with 2 drones + 1 EV, referred to as DT2, investigates the system's environmental and cost implications when drone deployment is increased. Meanwhile, the configurations of 2 electric trucks (ET) and 2 fuel trucks (FT) act as control groups, representing fully ground-based delivery modes. These fully ground-based configurations provide a benchmark for assessing the relative performance of conventional vehicles compared to drone-vehicle parallel systems. Regarding parameter settings, the vehicles' speed limit was fixed at 80 km/h in accordance with local traffic regulations. To reflect the frequent starting and stopping inherent to last-mile delivery in residential areas, the acceleration factor was set at 1.5. Figures A1–A3 in Appendix B illustrate representative instance plots for each fleet combination, showcasing how delivery tasks are allocated and executed.

**Table 5.** Drone and truck fleet combinations.

No.	Number of Trucks (Electric/Fuel)	Number of Drones
DT1	1 (Electric)	1
DT2	1 (Electric)	2
ET	2 (Electric)	0
FT	2 (Fuel)	0

#### (2) Delivery density

Delivery density significantly influences the operational efficiency and service quality in the parallel transportation system involving drones and trucks. In areas with high delivery density, the clustering of customer nodes enhances the scheduling efficiency of UAVs and lowers transportation costs. Conversely, in low delivery density regions, resource utilization may decrease, leading to higher operational costs and reduced service coverage. To examine this effect, this study selects two exemplar delivery densities: 20 deliveries/km<sup>2</sup> in urban suburbs and 1 delivery/km<sup>2</sup> in rural areas, based on the findings of [11]. Customer nodes are generated randomly within a circular area of a given radius. The choice of the radius  $r$  is critical because it directly determines the size of the area served by drones and affects vehicle scheduling and allocation decisions. Larger  $r$  values imply that customers are distributed farther from the distribution center, aligning the problem characteristics

more closely with the Vehicle Routing Problem (VRP). In contrast, smaller  $r$  values allow UAVs to serve more customers in closer proximity, making the problem resemble the Drone Delivery Routing Problem (DDRP). This study selects two specific radii values,  $r = 1.5$  and  $r = 5.5$ , corresponding to the two chosen delivery densities. These settings enable an in-depth evaluation of how density affects resource allocation, scheduling efficiency, and cost-effectiveness.

### (3) Traffic congestion and wind conditions

Traffic congestion significantly influences the average speed of vehicles, thereby directly affecting distribution efficiency. To comprehensively evaluate its impact on vehicle operations, this study categorizes vehicle speeds into three traffic congestion levels: low, medium, and high. Similarly, wind speed plays a critical role in determining the flight speed, range, and battery consumption of drones. Properly defining wind speed variables is essential to accurately analyze drone performance under varying meteorological conditions. Consequently, this study sets three wind scenarios—no wind, low wind, and high wind—to capture the effects of wind speed on UAV flight performance. These settings are based on the framework proposed by [7] and are detailed in Table 6.

**Table 6.** Parameter settings in experimental design for traffic and wind conditions.

Level	Traffic Congestion		Wind Conditions Mean Wind Speed $v_{wind}$ (km/h)
	Travel Speed $v_G$	Accel. Frequency Coefficient $n^{acc}$	
Low	$1 \cdot v_{rl}$	$0.5 \cdot n^{acc}$	0
Medium	$0.95 \cdot v_{rl}$	$1 \cdot n^{acc}$	25
High	$0.67 \cdot v_{rl}$	$2 \cdot n^{acc}$	45

### (4) Environmental and Cost Contexts

The structure of electricity production plays a crucial role in determining operational-phase emissions, as the CO<sub>2</sub>e produced per kWh of electricity can vary greatly depending on the energy sources used. Additionally, the cost structure of each country can significantly influence long-term economic viability. To evaluate the environmental and economic outcomes under varying electricity production and cost structures, this study considers two country contexts: Country 1, characterized by high-carbon electricity production (primarily coal and natural gas-based) and relatively low energy and labor costs, and Country 2, defined by low-carbon electricity production (mainly nuclear and renewable energy) alongside relatively high energy and labor costs. The costs of electricity, oil, and labor in these contexts are influenced by geographic and economic factors. For example, developing countries with limited electricity infrastructure may experience lower overall operating costs despite reduced energy and labor expenses, whereas developed countries often exhibit stable electricity prices despite higher oil and labor costs. These differences underline the necessity of tailoring operational strategies to specific regional characteristics. Details of the electricity production structure, energy, and labor costs for both country contexts are summarized in Table 7.

**Table 7.** Parameter settings in experimental design for country conditions.

Country Number	Emissions Emitted per Unit of Electricity (kg – CO <sub>2</sub> /kWh)	Energy Cost		Labor Cost	
		Fuel Cost (Yuan/L)	Electricity Cots (Yuan/kWh)	Driver Salary (Yuan/h)	Drone Operator Salary (Yuan/h)
Country 1	0.684	7.02	0.8	60	150
Country 2	0.056	14.15	1.49	109.29	196.55

In summary, this study explores the impact of various parameters on experimental outcomes through a systematically designed set of experimental scenarios. These include variations in customer densities (defined by different radius settings), wind speed conditions, traffic congestion levels, and environmental and cost contexts. Specifically, a total of  $2 \times 3 \times 3 \times 2 = 36$  experimental scenarios were developed. To ensure reliability and account for the effects of randomness, each scenario was repeated 50 times, with random generation of customer locations and demands within predefined constraints. This approach accounts for the inherent uncertainty in delivery tasks. Additionally, sensitivity analyses were conducted to evaluate the influence of the aforementioned critical parameters.

## 6.2. Performance of the Improved ALNS

The computational experiments were conducted on a hardware environment comprising an AMD Ryzen™ 5 7500F CPU with a clock speed of 3.7 GHz, 32 GB of RAM, and a 64-bit Windows 11 operating system. The solutions were implemented using Python, with the ALNS algorithms modified and optimized to evaluate their effectiveness and accuracy.

For comparative analysis, this study assesses the performance of the improved ALNS algorithm using six standard TSP benchmark instances: att48, berlin52, eil101, gr120, pr152, and gr229, along with 14 PDSTSP instances generated from 15 different settings for each TSP instance. The set of 84 instances, with customer numbers ranging from 48 to 229, was originally introduced in [27]. It is important to note that instances involving two depots are excluded, as the model considered in this study is specifically designed for scenarios with only one depot. In addition, RRLS [12] and HACO [63] are selected as benchmark algorithms for the PDSTSP. The specific 14 instances used are provided in Table 8.

**Table 8.** Experimental instances.

No.	Instances	The Percentage of Drone-Eligible Customers	The Drone Speed	Number of Drones
1	80-2-1	80	2	1
2	0-2-1	0	2	1
3	20-2-1	20	2	1
4	40-2-1	40	2	1
5	60-2-1	60	2	1
6	100-2-1	100	2	1
7	80-1-1	80	1	1
8	80-3-1	80	3	1
9	80-4-1	80	4	1
10	80-5-1	80	5	1
11	80-2-2	80	2	2
12	80-2-3	80	2	3
13	80-2-4	80	2	4
14	80-2-5	80	2	5

The results in Table 9 are the averaged outcomes across 14 instances for each of the six main problem categories, where the improved ALNS algorithm was executed randomly 10 times per instance. These averages provide a comprehensive view of the algorithm's performance across different scales, capturing both solution quality and runtime efficiency. The experimental results, summarized in Table 9, demonstrate the robust performance of the improved ALNS algorithm across various problem instances. For small-scale instances (att48 and berlin52), the improved ALNS achieves the optimal solutions, matching the results of HACO and RRLS, while its runtime is approximately 90% shorter than RRLS and only slightly higher than HACO. For medium-scale instances (eil101 and gr120), the improved ALNS provides solutions within 0.2% to 0.5% of HACO's results and better

than RRLS, though its runtime is about 150% to 170% longer than HACO, but still 60% shorter than RRLS. In large-scale instances (pr152 and gr229), the improved ALNS delivers solutions within 0.3% to 1% of HACO and RRLS, while its runtime is 35% to 40% shorter than RRLS and about 2–6 times longer than HACO. Although HACO excels in computational efficiency, the improved ALNS strikes a better balance between solution quality and runtime, demonstrating an approximate 50% to 90% reduction in runtime compared to traditional ALNS. These results highlight its strong adaptability and efficiency, making it an effective tool for both small and large-scale logistical optimization challenges.

**Table 9.** Results of the algorithms on the instance from [27].

Instance	Improved ALNS		HACO		RRLS	
	Result	Runtime(s)	Result	Runtime(s)	Result	Runtime(s)
att48	31,078.92	10.91	31,078.92	0.07	31,078.92	163.21
berlin52	6554.38	11.37	6554.38	2.58	6554.38	363.43
Eil101	533.03	68.63	532.11	27.22	532.08	430.01
gr120	1351.59	162.02	1351.59	59.82	1354.27	396.35
pr152	73,262.42	285.19	72,547.09	44.45	72,548.99	535.02
gr229	1708.73	457.22	1706.88	175.18	1709.91	633.58

The scalability of the improved ALNS algorithm is evident in its consistent performance across small- to medium-sized instances. However, as problem size increases, the algorithm exhibits a noticeable rise in computational requirements, indicating a potential scalability limitation. While solution quality remains robust, the increasing runtime suggests that the algorithm may face inefficiencies when addressing very large-scale instances.

### 6.3. Life Cycle Assessment Results

The following sections provide a comprehensive evaluation of the parallel transportation systems, examining their lifecycle environmental impacts and economic performance. The analysis focuses on three key evaluation metrics: lifecycle carbon emissions, noise pollution, and lifecycle costs, while also incorporating a sensitivity analysis of critical factors such as traffic congestion levels, delivery density, and wind speed conditions to assess their effects on emissions and costs. The study further compares the systems across two distinct contexts with differing electricity production methods and cost structures, highlighting the significant role of carbon intensity and economic variability.

#### 6.3.1. Overall Environmental Assessment

Figures 6 and 7 illustrate the carbon emission performance under different scenarios, with Figure 6 representing country 1 and Figure 7 representing country 2. (In the country 2 scenario, due to the high emissions and costs associated with the FT fleet, two breakpoints are applied to the y-axis in Figure 7 to better illustrate the data discrepancies. This may cause the error bars for the FT fleet to appear longer; however, this reflects the inherently higher values and broader error margins associated with this fleet.) The results highlight the significant environmental benefits of the parallel transportation system, particularly in reducing carbon emissions. Specifically, the study demonstrates that the parallel transportation reduces carbon emissions by approximately 20% compared to the ET combination. Among the various combinations, the DT2 combination performs particularly well, effectively covering a larger operational area with minimal energy consumption and emissions. This advantage is most pronounced in the DT1 and DT2 combinations, where the drones' low energy consumption and emissions allow them to efficiently take on more tasks within their operational range. However, in country 1, which has a high-carbon electricity production structure, the FT combination produces the lowest carbon emissions

in low-density areas. This finding underscores the significant impact of the electricity production structure on emissions. In terms of noise pollution, the ET combination emerges as the best performer, producing significantly lower noise levels compared to the other combinations. On the contrary, the DT1 combination generates a more concentrated and higher noise level, while the DT2 combination, with its additional drones, results in even greater noise impacts.

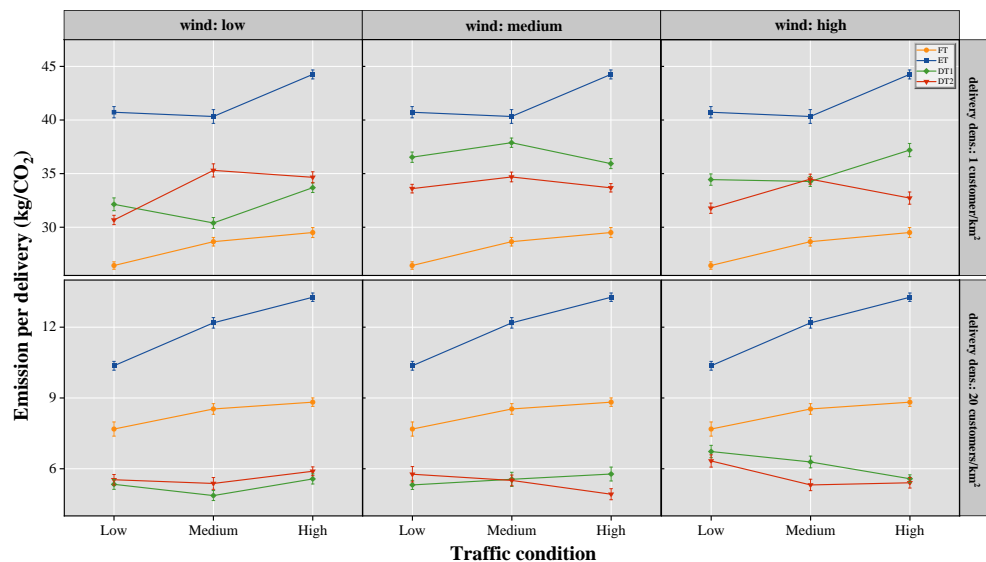


**Figure 6.** kgCO<sub>2</sub>/delivery in country 1.

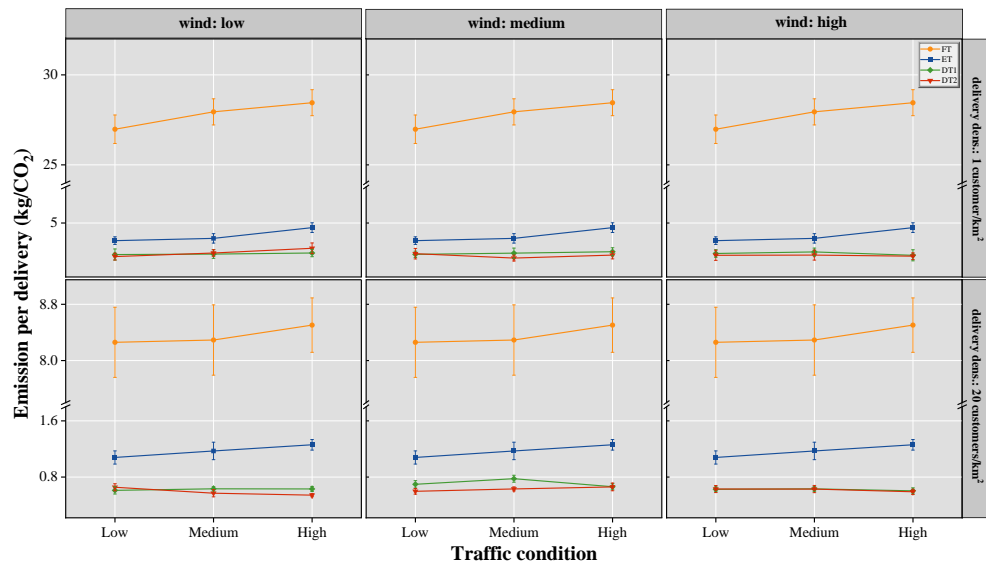


**Figure 7.** kgCO<sub>2</sub>/delivery in country 2.

### 6.3.2. Emission Impacts

Due to the numerous combinations of experimental scenarios, it is difficult to fully address all contexts for each life cycle phase. To ensure the representativeness and applicability of the research results, we selected a typical and representative experimental scenario for in-depth analysis. First, we chose a medium traffic congestion condition, which is relatively common in urban logistics and distribution and reflects the typical conditions in most urban areas. Second, we selected 1 delivery/km<sup>2</sup>. A lower delivery density allows for a more comprehensive demonstration of the performance and efficiency of different fleet combinations across a broader area. Additionally, we selected windless conditions. In

the absence of wind, the wind speed factor has minimal impact on the analyzed results, allowing the experiment to focus on comparing the performance of the vehicles and drones, while minimizing the interference of environmental factors.

Figures 8 and 9 present a breakdown of emissions for each system. The results indicate that the drone-truck parallel system achieves significantly lower emissions during the operational phase compared to other systems, with operational emissions accounting for approximately 97% of its total emissions. Notably, the drone's contribution to operational emissions is minimal, comprising only about 2% of the total. In contrast, the conventional two-truck system generates over 99% of its total emissions during the operational phase. This highlights the effectiveness of the drone-assisted transportation model in reducing operational emissions, particularly due to the drones' lower energy consumption, which contributes to an overall reduction in emissions.

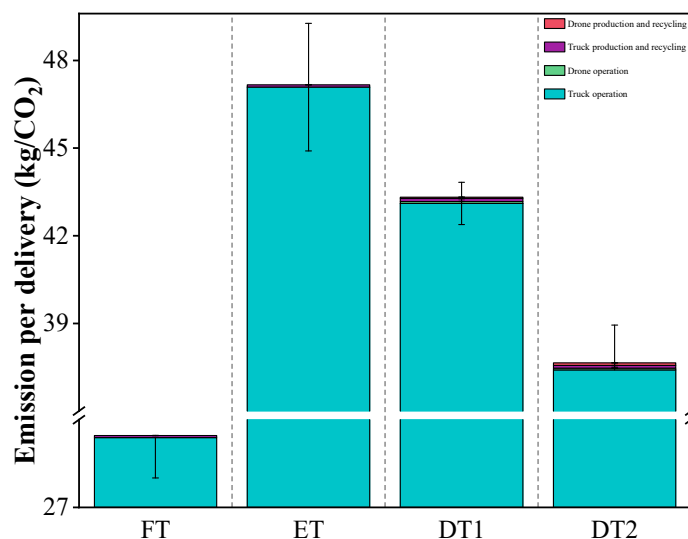


**Figure 8.** Emission breakdown in country 1.

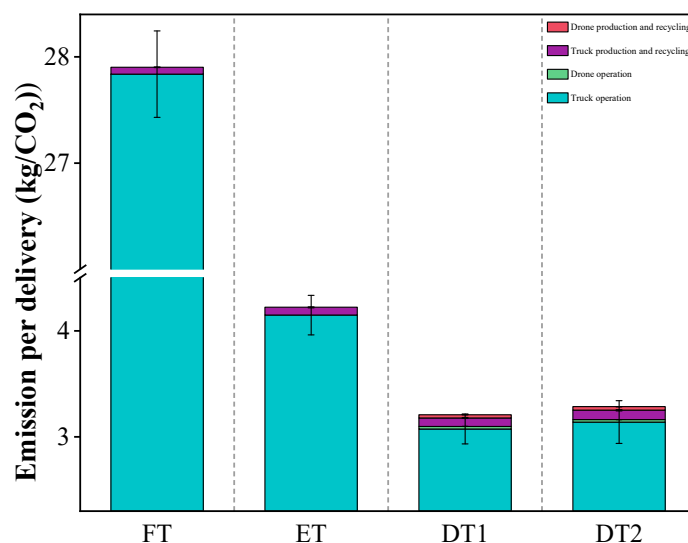


**Figure 9.** Emission breakdown in country 2.

However, the drone-truck parallel system exhibits relatively higher emissions during the production and recycling phases, primarily due to the manufacturing process of drones. Despite the increased production-phase emissions, these account for a negligible share of the total lifecycle emissions because of drones' shorter travel distances and low energy

usage. Operational-phase emissions remain the dominant factor in lifecycle emissions for trucks and drones, serving as the main driver of emission reductions. Detailed results for operational-phase emissions across different logistics scenarios are provided in Appendix A, demonstrating that delivery density and traffic conditions are key variables influencing emissions. Among secondary variables, wind speed has a relatively minor effect on energy consumption and emissions per delivery. However, under high wind conditions, drone emissions increase slightly by approximately 5–10%.

### 6.3.3. Noise Impacts

In the noise impact analysis, the scenario with a delivery radius of 5500 m is chosen due to the more complex noise propagation paths in larger distribution areas. In such scenarios, the number and distribution of noise sources are more representative of the surrounding environment, providing a more comprehensive analysis of the noise impact. To facilitate the calculation of noise distribution, the study divides the entire area into an 800-m grid. This gridded approach ensures a moderate spatial resolution, allowing for effective capturing and analysis of noise levels across different areas while maintaining calculation efficiency and accuracy. By analyzing the noise distribution, the study provides deeper insights into how various modes of transportation contribute to environmental noise in large-scale delivery scenarios. The Figure 10 illustrating the noise impact of different fleet combinations reveals significant differences in both the distribution and the levels of noise generated by each combination. These findings highlight the varying degrees of noise pollution produced by different fleet combinations and their potential environmental impact in urban and suburban delivery settings.

First, the noise performance of the 2-truck combination is more dispersed, due to the simultaneous operation of the two trucks, which results in the formation of multiple noise regions. The noise characteristics of this combination exhibit greater volatility, with significant variations in noise levels at different locations. Notably, the FT operates at a higher noise level, and its noise is more widely spread, causing greater noise impact on the surrounding environment. In contrast, the noise level of the ET is relatively low, and its impact on the environment is more contained. This is largely due to the quieter nature of electric vehicles, which do not generate as much noise as internal combustion engines.

In the DT1, the noise is primarily concentrated in the central area of the distribution zone. The UAV's engine and propeller become the dominant sources of noise, and this noise propagates farther than that of ground vehicles. The extended range of the UAV's noise significantly raises the noise level in the central area, with the sound spreading over a larger distance compared to the truck noise. The addition of drones alters the noise propagation pattern, so the noise level remains elevated even at longer distances from the source. This results in a broader environmental impact, making the overall noise level higher compared to combinations that rely solely on trucks.

In the DT2, the noise distribution became more even compared to the DT1. The addition of the second drone increased the number of noise sources, which led to a wider spread of noise. As a result, the overall noise level increased, and the environmental impact of noise extended over a larger area due to the additional UAV. The presence of the extra drone contributed to an increase in overall noise pollution.

In summary, the ET performed the best in the noise analysis, generating significantly lower noise levels compared to the other combinations. In contrast, the DT1 produced concentrated and high noise levels in the central delivery area, while the DT2 combination, though slightly noisier, distributes noise more evenly, reducing the impact in specific regions.

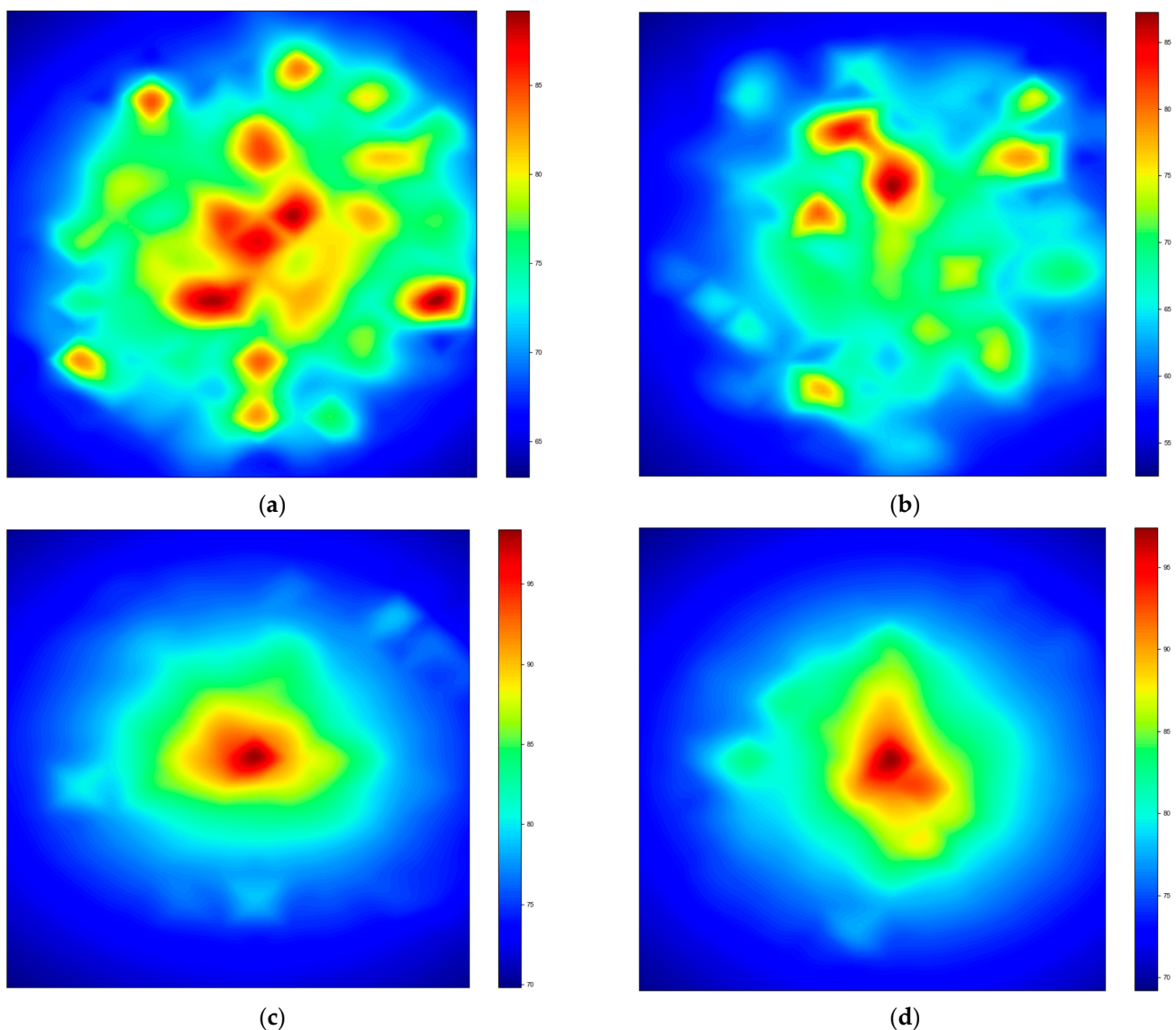


**Figure 10.** (a) Noise map of FT; (b) Noise map of ET; (c) Noise map of DT1; (d) Noise map of DT2.

#### 6.4. Life Cycle Cost Analysis Results

##### 6.4.1. Overall Cost Assessment

Figure 11 illustrates the cost performance of four fleet combinations for country 1, Figure 12 shows that for country 2. The results of the study indicate that the ET combination consistently offers the lowest overall costs across all scenarios. This demonstrates the economic advantages of electric vehicles, especially in long-term operation where energy efficiency and lower operating costs are key factors. In contrast, the FT combination has the highest costs, primarily due to its higher fuel expenses, which are more sensitive to fluctuations in oil prices. The DT1 and DT2 combinations have significantly lower costs compared to the FT with cost reductions ranging from approximately 20% to 30%. This advantage stems from the ability of drones to handle a portion of the delivery tasks, coupled with their cleaner energy sources, which lower energy consumption and operational costs. However, despite the cost savings from drones, their high initial investment costs and operational expenses (e.g., battery replacement and maintenance) make the overall cost of the DT1 and DT2 combinations slightly higher than the ET combination in some scenarios.

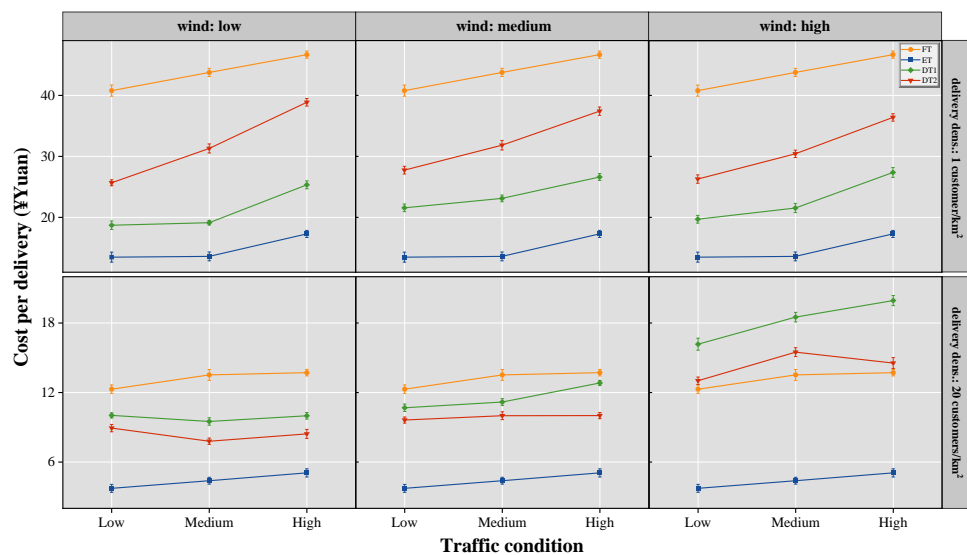


**Figure 11.** ¥Yuan/delivery in country 1.

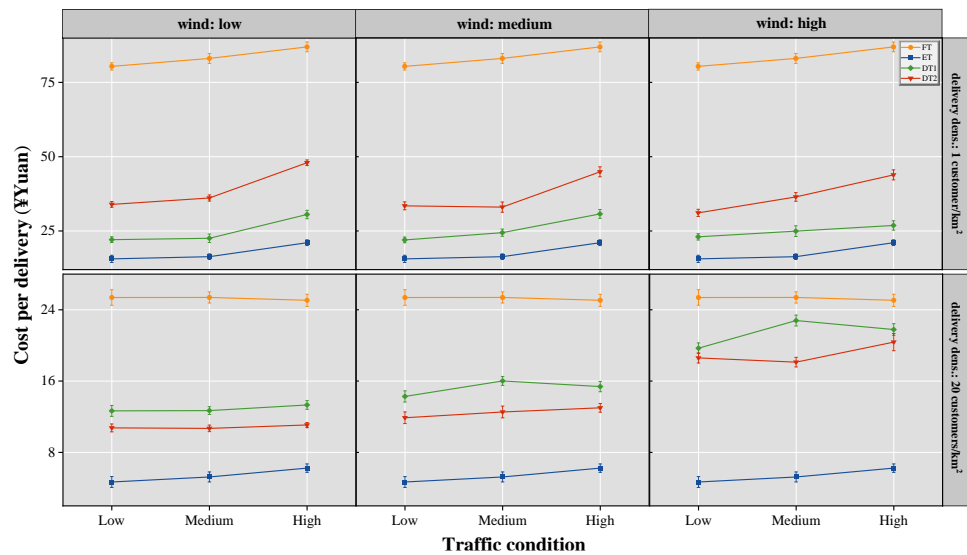


**Figure 12.** ¥Yuan/delivery in country 2.

#### 6.4.2. Cost Impacts

Figure 13 illustrates the cost breakdown for each fleet combination at each life cycle stage, providing a detailed comparison across the typical scenarios considered in the study. The analysis reveals significant differences in both initial and operational costs between different combinations. For the DT1 combination, the initial cost makes up a smaller percentage of the total cost, while the operational cost accounts for a much higher percentage of 65%. This suggests that the DT1 combination is cost-effective in terms of initial investment and energy consumption but incurs higher long-term operating and maintenance costs. The combination is efficient in terms of deployment and energy usage, but ongoing costs are a significant consideration, particularly for routine upkeep and the operation of drones. In contrast, the DT2 combination sees a rise in both initial and energy-related costs. Its operational costs increase further to 74%, driven by the higher costs associated with maintaining and operating two drones, particularly in high-density delivery areas where the drones are used more intensively.

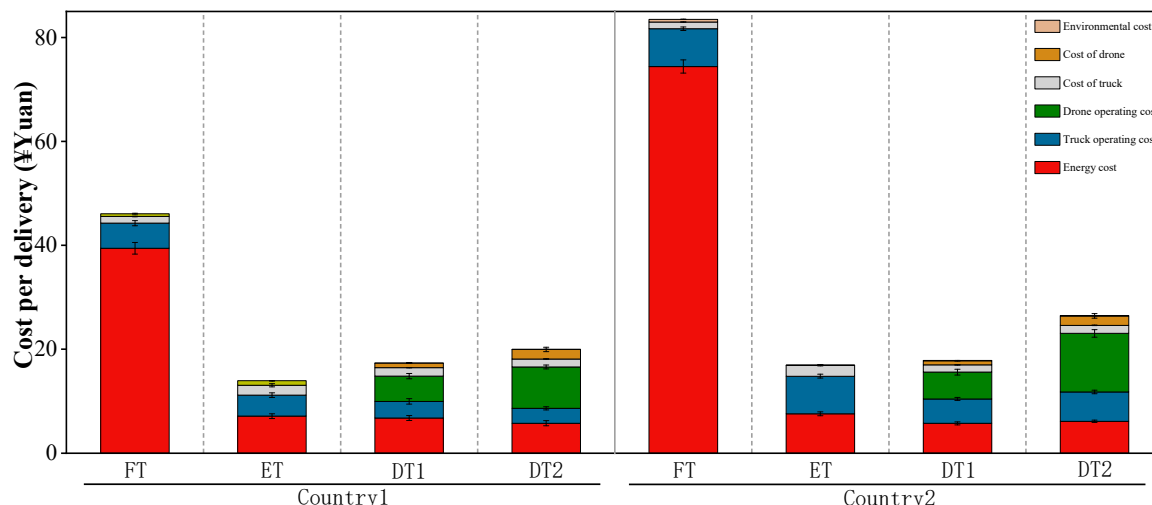


**Figure 13.** Cost breakdown.

Secondly, the energy cost difference between the ET and FT combinations is significant. In the FT, energy costs account for 89% of the total costs, reflecting the high fuel consumption of fuel trucks over a long operational period. This is not only due to the high fuel prices but also because fuel trucks have a much greater energy demand. As a result, despite relatively low initial and operating costs, energy costs make up the vast majority of the total costs. In contrast, the energy cost for the ET combination accounts for 45% of the total cost, with its initial costs and operating costs comprising 12% and 41%, respectively. This indicates that while the ET combination requires a higher initial investment, its energy cost efficiency is significantly better than that of the FT combination. Moreover, its operating and maintenance costs are relatively reasonable, which allows it to demonstrate a strong economic advantage over the long term. Furthermore, the operating costs of the DT1 and DT2 combinations are notably higher than those of the ET and FT combinations. This is largely due to the higher labor costs associated with UAV operations, as well as the additional costs related to airspace usage. In regions with stricter airspace management regulations, the costs for controlling UAVs in the airspace may further increase, making UAV operating costs significantly higher than those of traditional ground vehicles.

### 6.5. Sensitivity Analysis

Similar to the scenario described in Section 6.3.2, this sensitivity analysis evaluates the individual impacts of three parameters: delivery density, traffic conditions, and wind speed, while holding the remaining parameters constant at predefined baseline values of low delivery density, medium traffic congestion, and low wind speed. All analyses are conducted under the conditions of Country 2.

#### 6.5.1. Sensitivity Analysis of Delivery Density

Figures 14 and 15 illustrate the impact of delivery density on emissions and costs, highlighting clear trends across all transportation modes. Emissions show a substantial decrease as delivery density increases. For instance, emissions for fuel trucks drop by approximately 70%, and drone-integrated systems like DT2 experience a reduction of about 69%. This significant improvement is primarily due to shorter delivery distances, which result in reduced fuel or energy consumption. In high-density areas, delivery routes become more compact, allowing vehicles and drones to serve more customers per trip, which reduces idle running times and unnecessary energy usage.

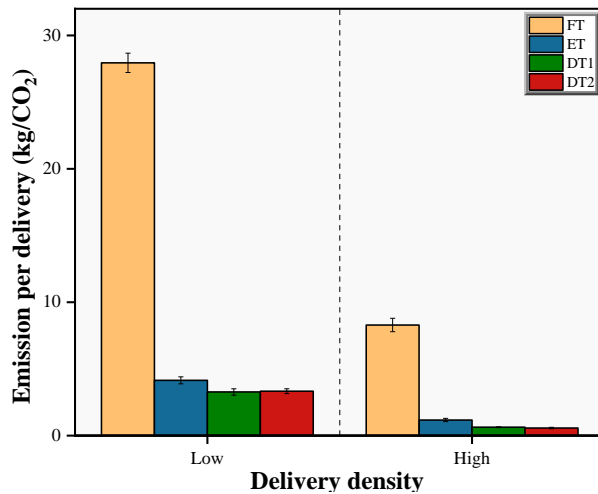


**Figure 14.** Impact of delivery density on emissions.

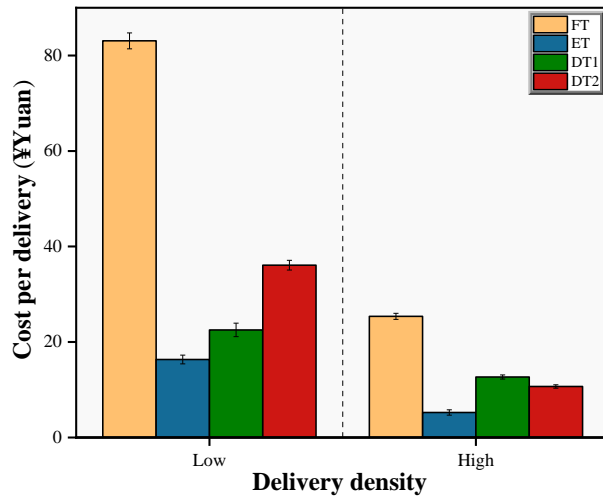


**Figure 15.** Impact of delivery density on costs.

Likewise, costs also decrease markedly with increasing delivery density, with reductions of around 70% observed across all modes. High-density delivery allows for better utilization of resources, as shorter travel distances reduce energy consumption and labor requirements. The parallel systems, particularly DT2, benefit the most in these scenarios. The use of two drones enables a more balanced workload, which reduces energy use and extends the operational life of equipment. High-density delivery leads to cost reductions primarily due to shorter travel distances, which lower energy costs.

#### 6.5.2. Sensitivity Analysis of Traffic Condition

Figures 16 and 17 illustrate the impact of varying traffic conditions on emissions and costs across different transportation modes. Traffic congestion significantly affects both metrics, with ground vehicle-based systems like FT and ET showing greater sensitivity than drone-integrated systems such as DT1 and DT2. As congestion increases, carbon emissions rise notably. Under moderate congestion, emissions for DT1 and DT2 increase by approximately 15%, while under high congestion, they rise by 20%. In comparison, ET emissions grow more significantly, by around 25% under high congestion, reflecting the system's reliance on road conditions. FT consistently shows the highest emissions across all congestion levels due to prolonged idling and inefficient fuel use. However, the parallel systems, especially DT2, maintain relatively stable and low emissions. This stability is

attributed to the system's ability to assign more delivery tasks to drones, which bypass traffic and reduce the dependence on ground vehicles.

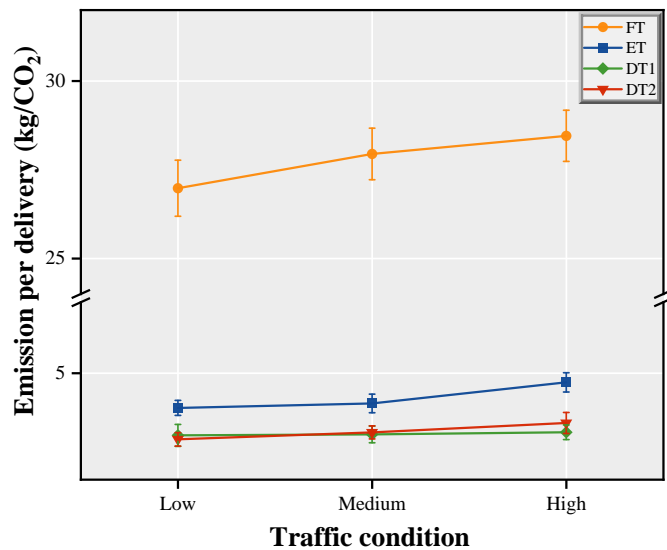


**Figure 16.** Impact of traffic condition on emissions.

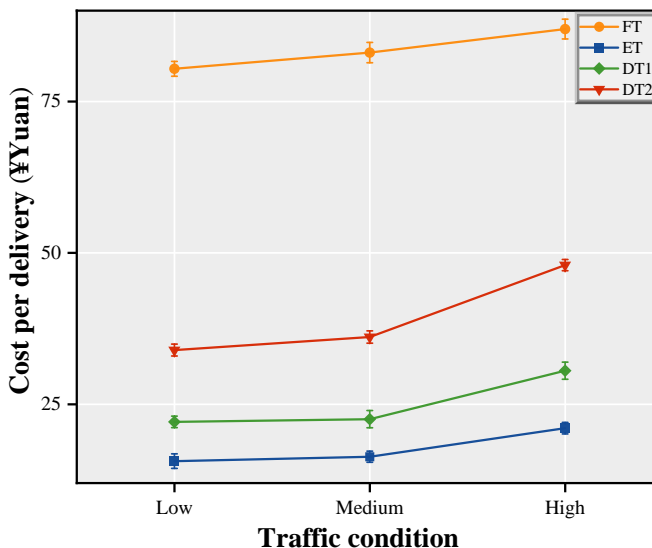


**Figure 17.** Impact of traffic condition on costs.

Costs follow a similar trend, with all modes experiencing increases as congestion worsens. FT and ET see cost increases of approximately 20% under high congestion, driven by slower travel speeds and longer delivery times. The parallel systems, however, show smaller cost increases. The use of UAVs mitigates the effects of congestion by reducing the time and distance required for vehicle-based deliveries. DT2, leveraging two drones for workload, proves particularly efficient in limiting cost escalations.

### 6.5.3. Sensitivity Analysis of Wind Conditions

Figures 18 and 19 illustrate the impact of varying wind conditions on emissions and costs across different transportation modes. Overall, the impact of wind speed on drone-based systems is relatively minor compared to other factors such as delivery density or traffic congestion. This analysis focuses on the impact of wind conditions on the parallel systems and does not consider the effects of wind on trucks, as these vehicles are minimally affected by wind speed.

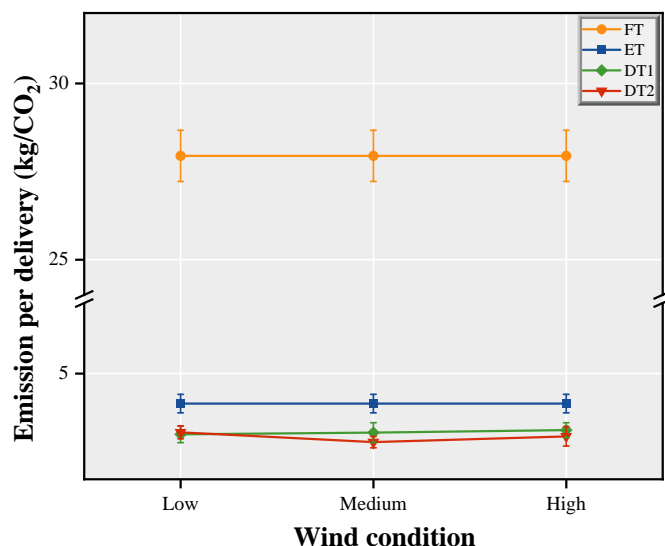


**Figure 18.** Impact of wind condition on emissions.

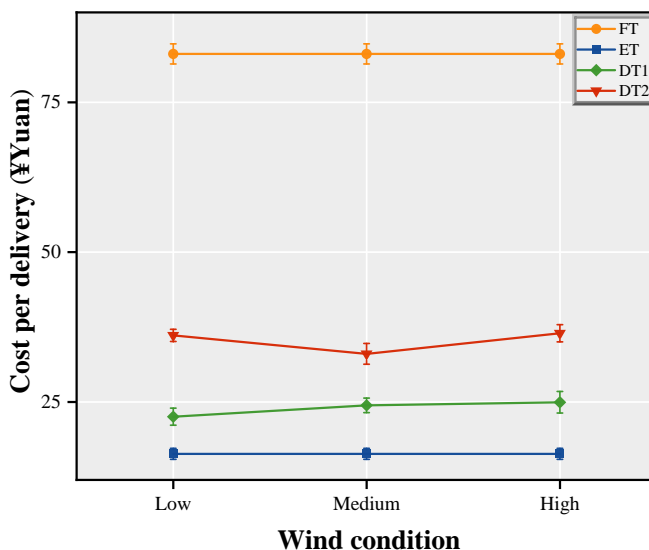


**Figure 19.** Impact of wind condition on costs.

As wind intensity increases, carbon emissions for drone systems rise slightly. As wind speed increases from low to high, emissions for DT1 and DT2 rise by approximately 5 to 10% due to the additional energy required to maintain flight stability in stronger winds. Despite this increase, drones continue to demonstrate significantly lower emissions compared to ground-based systems, maintaining their environmental efficiency even under challenging wind conditions.

Costs also follow an upward trend as wind speed increases. Higher wind speeds lead to increased energy consumption as drones work harder to maintain stability during flight, directly raising energy costs. As wind conditions worsen, the additional energy required to counteract wind resistance results in noticeable cost escalations.

#### 6.5.4. Comparison of Two Different Environmental and Economic Conditions

Figures 20 and 21 highlight the differences in emissions and costs across transportation modes under the contrasting conditions of Country 1 and Country 2. These variations are influenced by the carbon intensity of electricity, as well as differences in energy and labor costs.

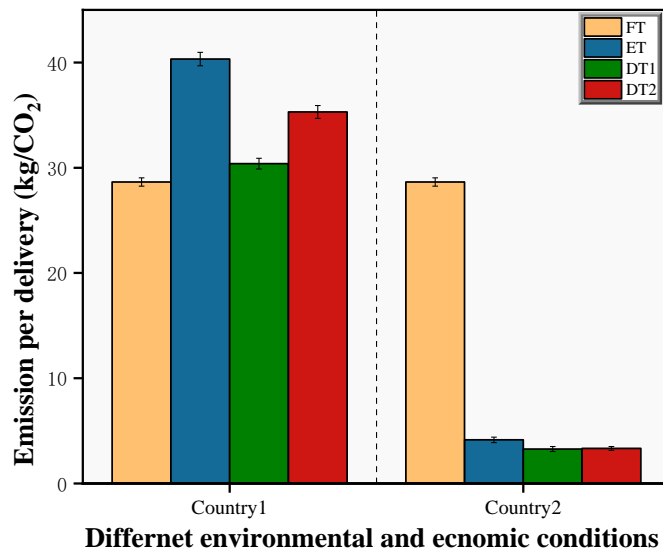


**Figure 20.** Emissions comparison of Country 1 and Country 2.

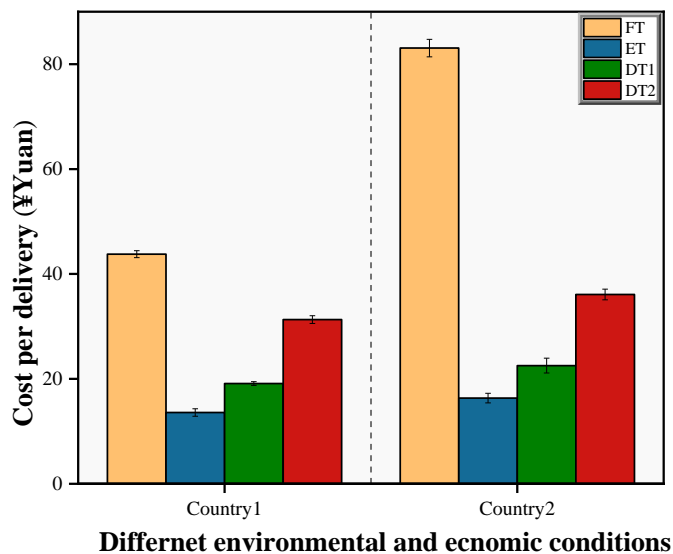


**Figure 21.** Costs Comparison of Country 1 and Country 2.

In Country 1, the high-carbon electricity production results in significantly higher emissions for ET, DT1, and DT2 compared to Country 2. For instance, emissions for ET in Country 1 are approximately 10 times higher than in Country 2, and DT2 emissions are over 8 times higher due to reliance on fossil-fuel-based electricity. Notably, in Country 1, FT even achieves the lowest emissions among all modes, as it is not affected by the carbon intensity of electricity production. In contrast, in Country 2, emissions for ET and drone systems are drastically reduced, with ET achieving 50% lower emissions compared to Country 1, highlighting the critical role of low-carbon energy in enabling environmentally efficient logistics systems.

Costs in Country 1 are lower for all modes due to cheaper fuel and labor. However, in Country 2, the higher energy and labor costs increase the operational expenses for FT, making it up to 20% more expensive than in Country 1. ET, DT1, and DT2 are less affected by these cost increases due to the efficiency of low-carbon electricity. For the parallel systems, the cost difference between the two countries remains stable at around 10 to 15%, highlighting their economic viability even in high-cost contexts.

### 6.6. Discussion

The experimental results demonstrate that the parallel drone-truck transportation system offers significant benefits in both environmental and economic aspects. Based on the analysis of the results, several suggestions are proposed to address the challenges in both government management and operational management, which are essential to fully realizing these benefits and ensuring long-term sustainability.

From a government management perspective, addressing these challenges requires a thorough understanding of their impacts. A full lifecycle assessment is essential to systematically quantify emissions and environmental effects, ensuring both production phase and operational emissions are accurately evaluated and addressed. This approach prevents an overemphasis on operational emissions, which may underestimate the true environmental impact of emerging technologies like drones. Regarding noise pollution, while drones generate more noise compared to traditional ground vehicles, the solution lies in managing this issue in a sound and balanced manner. Governments can introduce noise standards specifically tailored for drone operations and regulate their flight schedules in urban environments to limit noise pollution effectively. Such measures can help mitigate the negative impact on residents in densely populated areas, ensuring a harmonious integration of drones into urban transportation systems.

From an operational management perspective, addressing the challenge of quantifying the long-term costs of the transportation system requires a focus on both current expenses and future efficiencies. While drones currently incur higher costs for procurement, maintenance, and battery replacement, advances in technology are likely to reduce these costs over time [45]. Investing in research and development to enhance drone efficiency, extend battery life, and lower maintenance expenses is a critical strategy for operators. Furthermore, operators can achieve better cost efficiency by utilizing the parallel system in high-density urban areas, where it offers higher economic benefits. However, in regions with low electricity and labor costs, using electric trucks alone is more cost-effective.

Additionally, the energy structure of a region significantly influences emissions. In regions where clean energy sources like wind and solar power are abundant, the carbon emissions of drones and electric vehicles can be significantly lower. Operators, together with governments, should focus on transitioning to renewable energy sources to enhance the system's environmental sustainability.

## 7. Conclusions

### 7.1. Summary

This study investigates the environmental and economic impacts of drone and truck parallel transportation over the lifecycle. First, a parallel transportation model was developed, where deliveries are completed jointly by a truck and one or more drones. The environmental impact is assessed using a comprehensive LCA method, quantifying emissions at each stage and analyzing noise during transportation. On the economic side, LCCA evaluates costs across five components, considering energy, environmental liability, and other factors. Sensitivity analysis explores delivery density, traffic congestion, and wind speed, comparing results in two countries under different environmental and cost contexts. Additionally, sensitivity analysis explores delivery density, traffic congestion, and wind speed, by comparing results in two countries under different environmental and cost contexts. Simulations using an improved ALNS algorithm indicate that the parallel transportation system can reduce carbon emissions by approximately 20% compared to electric trucks alone. While electric trucks produce the least noise, the parallel system generates higher noise levels due to drone operations. In terms of costs, fuel trucks incur the highest expenses, mainly driven by fuel costs. The parallel system, in contrast, offers

significant cost savings ranging from 20% to 30% compared to fuel trucks, largely due to the lower operating costs of drones. However, the high initial investment and maintenance costs associated with drones result in the parallel system's total cost being slightly higher than that of electric trucks. The system's performance is also strongly influenced by the region's energy structure. In areas with abundant renewable energy, both drones and electric trucks offer greater environmental benefits and lower costs.

## 7.2. Future Study

Despite the comprehensive analysis, several limitations warrant future investigation. First, the applicability of certain assumptions to real-world contexts requires validation. For instance, the assumption of one delivery per destination may not apply in cases like multi-story apartments, where trucks can enhance efficiency through multiple deliveries at a single location. Simplified logistics parameters, such as constant truck speed and straight drone flight paths, overlook real-world complexities like risk aversion and environmental factors, including wind direction, which significantly impact drone performance and energy consumption.

To address these limitations, future research can incorporate more realistic constraints, including considerations for multiple depots, return logistics, and drone charging limitations. Comparative studies on delivery configurations, such as mobile truck-drone systems versus fixed parallel drone deployments, could provide valuable insights into their relative efficiency under varying conditions. Expanding environmental assessments to include indicators such as air quality and ecological impacts would enhance the comprehensiveness of the analysis. On the economic side, future studies can emphasize balancing costs and benefits rather than focusing solely on cost reduction. Investigating optimal drone-to-truck ratios in different operational environments (urban, suburban, rural) could yield actionable insights. Additionally, exploring advancements in energy efficiency will be crucial for improving the sustainability and effectiveness of systems.

**Author Contributions:** Conceptualization, D.B. and Y.Y.; methodology, D.B. and Y.Y.; software, Y.Y.; investigation, D.B., Y.Y. and J.C.; writing—original draft preparation, D.B. and Y.Y.; writing—review and editing, D.B. and Y.L.; funding acquisition, D.B. All authors have read and agreed to the published version of the manuscript.

**Funding:** This research was funded by State Key Laboratory of Air Traffic Management System (grant number SKLATM202406).

**Data Availability Statement:** Data are contained within the article.

**Acknowledgments:** The authors wish to express their sincere gratitude to the editor and the anonymous reviewers for their insightful comments and constructive feedback, which have significantly contributed to the improvement and clarification of this manuscript.

**Conflicts of Interest:** The authors declare no conflicts of interest.

## Appendix A. Emissions Breakdown per Scenario for Each Combination

**Table A1.** Emissions breakdown per scenario for each combination.

Traffic			Wind Speed			Radius (m)		Production and Recycling Phase 1				Use Phase 1			Overall Emissions 1					
Low	Medium	High	Low	Medium	High	1500	5500	ET	FT	DT1	DT2	ET	FT	DT1	DT2	ET	FT	DT1	DT2	
X	X		X					X	0.074	0.066	0.083	0.092	4.045	27.923	3.063	3.258	4.119	27.989	3.146	3.35
		X		X				X	-11%	-11%	-4%	-8%	-4%	-4%	4%	0%	-4%	-4%	3%	0%
		X	X					X	43%	31%	44%	37%	9%	2%	11%	7%	10%	2%	8%	4%
	X			X				X	0%	0%	6%	-9%	0%	0%	4%	2%	0%	0%	4%	0%
X				X				X	0%	0%	11%	0%	0%	0%	9%	0%	0%	0%	10%	0%
X		X			X			-65%	-64%	-31%	-69%	-72%	-70%	-81%	-83%	-72%	-70%	-80%	-83%	

<sup>1</sup> = measured in kgCO<sub>2</sub>e/delivery.

The table presents emissions data for different scenarios (Traffic, Wind Speed, Radius) across various phases (Production and Recycling, Use, Overall). The first row represents the baseline data, and the “X” marks in the table indicate different parameter values under each specific scenario. Positive and negative percentages show the relative change in emissions compared to the baseline for each case.

## Appendix B. Instance Plots

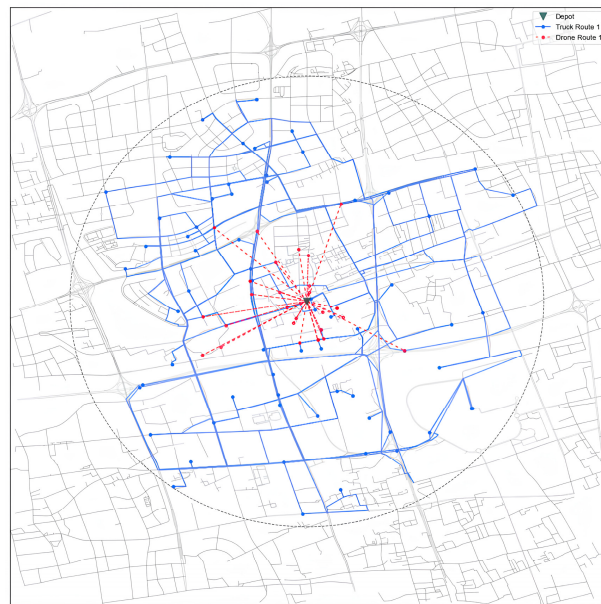


**Figure A1.** DT1 example.

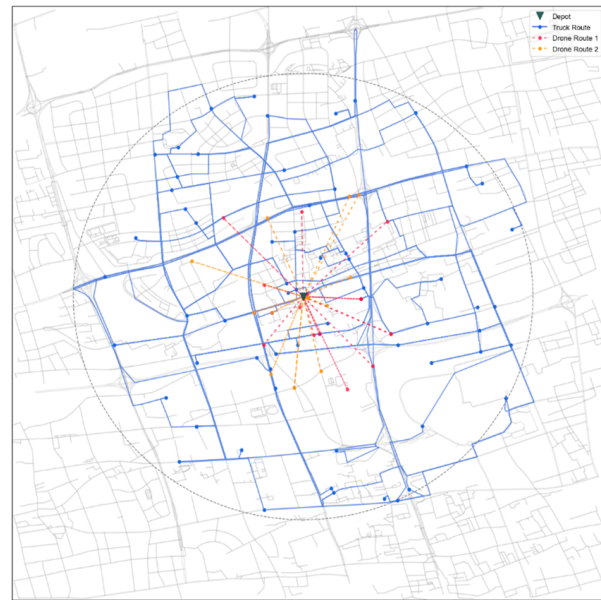


**Figure A2.** DT2 example.

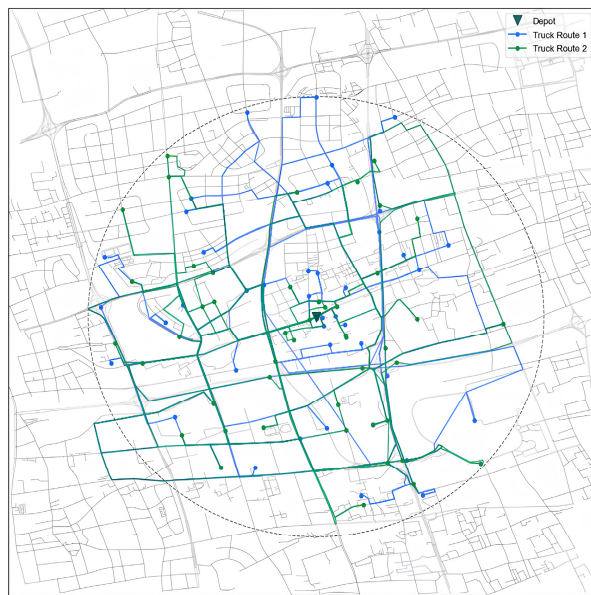


**Figure A3.** FT/ET example.

## References

1. Joerss, M.; Schroder, J.; Neuhaus, F.; Klink, C.; Mann, F. Parcel Delivery. In *The Future of Last Mile*; McKinsey & Company: New York, NY, USA, 2016.
2. Tavana, M.; Khalili-Damghani, K.; Santos-Arteaga, F.J.; Zandi, M.-H. Drone Shipping versus Truck Delivery in a Cross-Docking System with Multiple Fleets and Products. *Expert Syst. Appl.* **2017**, *72*, 93–107. [CrossRef]
3. Ham, A.M. Integrated Scheduling of M-Truck, m-Drone, and m-Depot Constrained by Time-Window, Drop-Pickup, and m-Visit Using Constraint Programming. *Transp. Res. Part C Emerg. Technol.* **2018**, *91*, 1–14. [CrossRef]
4. Teal Group, Teal Group Predicts Worldwide Civil Drone Production Will Almost Triple over the Next Decade. Available online: <https://www.tealgroup.com/index.php/pages/press-releases/60-teal-group-predicts-worldwide-civil-drone-production-will-almost-triple-over-the-next-decade> (accessed on 4 November 2023).
5. Goodchild, A.; Toy, J. Delivery by Drone: An Evaluation of Unmanned Aerial Vehicle Technology in Reducing CO<sub>2</sub> Emissions in the Delivery Service Industry. *Transp. Res. Part D Transp. Environ.* **2018**, *61*, 58–67. [CrossRef]
6. Kim, E. The Most Staggering Part About Amazon's Upcoming Drone Delivery Service. Available online: <https://businessinsider.com/cost-savings-from-amazon-drone-deliveries-2016-6> (accessed on 12 December 2023).
7. Kirschstein, T. Comparison of Energy Demands of Drone-Based and Ground-Based Parcel Delivery Services. *Transp. Res. Part D Transp. Environ.* **2020**, *78*, 102209. [CrossRef]
8. Guinée, J.B.; Heijungs, R.; Huppens, G.; Zamagni, A.; Masoni, P.; Buonamici, R.; Ekwall, T.; Rydberg, T. Life Cycle Assessment: Past, Present, and Future. *Environ. Sci. Technol.* **2011**, *45*, 90–96. [CrossRef]
9. Figliozi, M.A. Lifecycle Modeling and Assessment of Unmanned Aerial Vehicles (Drones) CO<sub>2</sub>e Emissions. *Transp. Res. Part D Transp. Environ.* **2017**, *57*, 251–261. [CrossRef]
10. D'Andrea, R. Guest editorial: Can drones deliver? *IEEE Trans. Autom. Sci. Eng.* **2014**, *11*, 647–648. [CrossRef]
11. Baldisseri, A.; Siragusa, C.; Seghezzi, A.; Mangiaracina, R.; Tumino, A. Truck-Based Drone Delivery System: An Economic and Environmental Assessment. *Transp. Res. Part D Transp. Environ.* **2022**, *107*, 103296. [CrossRef]
12. Dell'Amico, M.; Montemanni, R.; Novellani, S. Matheuristic Algorithms for the Parallel Drone Scheduling Traveling Salesman Problem. *Ann. Oper. Res.* **2020**, *289*, 211–226. [CrossRef]
13. Meng, Z.; Zhou, Y.; Li, E.Y.; Peng, X.; Qiu, R. Environmental and Economic Impacts of Drone-Assisted Truck Delivery under the Carbon Market Price. *J. Clean. Prod.* **2023**, *401*, 136758. [CrossRef]
14. Saleu, R.G.M.; Deroussi, L.; Feillet, D.; Grangeon, N.; Quilliot, A. The Parallel Drone Scheduling Problem with Multiple Drones and Vehicles. *Eur. J. Oper. Res.* **2022**, *300*, 571–589. [CrossRef]
15. Murray, C.C.; Chu, A.G. The Flying Sidekick Traveling Salesman Problem: Optimization of Drone-Assisted Parcel Delivery. *Transp. Res. Part C Emerg. Technol.* **2015**, *54*, 86–109. [CrossRef]
16. Agatz, N.; Bouman, P.; Schmidt, M. Optimization Approaches for the Traveling Salesman Problem with Drone. *Transp. Sci.* **2018**, *52*, 965–981. [CrossRef]
17. Bouman, P.; Agatz, N.; Schmidt, M. Dynamic Programming Approaches for the Traveling Salesman Problem with Drone. *Networks* **2018**, *72*, 528–542. [CrossRef]

18. Tu, P.A.; Dat, N.T.; Dung, P.Q. Traveling Salesman Problem with Multiple Drones. In Proceedings of the 9th International Symposium on Information and Communication Technology, Da Nang, Vietnam, 6–7 December 2018; pp. 46–53.
19. Murray, C.C.; Raj, R. The Multiple Flying Sidekicks Traveling Salesman Problem: Parcel Delivery with Multiple Drones. *Transp. Res. Part C Emerg. Technol.* **2020**, *110*, 368–398. [\[CrossRef\]](#)
20. Mara, S.T.W.; Rifai, A.P.; Sopha, B.M. An Adaptive Large Neighborhood Search Heuristic for the Flying Sidekick Traveling Salesman Problem with Multiple Drops. *Expert Syst. Appl.* **2022**, *205*, 117647. [\[CrossRef\]](#)
21. Boccia, M.; Mancuso, A.; Masone, A.; Murino, T.; Sterle, C. New Features for Customer Classification in the Flying Sidekick Traveling Salesman Problem. *Expert Syst. Appl.* **2024**, *247*, 123106. [\[CrossRef\]](#)
22. Dorling, K.; Heinrichs, J.; Messier, G.G.; Magierowski, S. Vehicle Routing Problems for Drone Delivery. *IEEE Trans. Syst. Man Cybern. Syst.* **2017**, *47*, 70–85. [\[CrossRef\]](#)
23. Savuran, H.; Karakaya, M. Efficient Route Planning for an Unmanned Air Vehicle Deployed on a Moving Carrier. *Soft Comput.* **2016**, *20*, 2905–2920. [\[CrossRef\]](#)
24. Campbell, J.F.; Sweeney, D.; Zhang, J. (Eds.) *Strategic Design for Delivery with Trucks and Drones*; Supply Chain Anal. Report. SCMA-2017-0201; College of Business Administration, University of Missouri: St. Louis, MO, USA, 2017.
25. Lei, D.; Chen, X. An Improved Variable Neighborhood Search for Parallel Drone Scheduling Traveling Salesman Problem. *Appl. Soft Comput.* **2022**, *127*, 109416. [\[CrossRef\]](#)
26. Nguyen, M.A.; Dang, G.T.-H.; Hà, M.H.; Pham, M.-T. The Min-Cost Parallel Drone Scheduling Vehicle Routing Problem. *Eur. J. Oper. Res.* **2022**, *299*, 910–930. [\[CrossRef\]](#)
27. Saleu, R.G.M.; Deroussi, L.; Feillet, D.; Grangeon, N.; Quilliot, A. An Iterative Two-step Heuristic for the Parallel Drone Scheduling Traveling Salesman Problem. *Networks* **2018**, *72*, 459–474. [\[CrossRef\]](#)
28. González, R.P.L.; Canca, D.; Andrade-Pineda, J.L.; Calle, M.; Leon-Blanco, J.M. Truck-Drone Team Logistics: A Heuristic Approach to Multi-Drop Route Planning. *Transp. Res. Part C Emerg. Technol.* **2020**, *114*, 657–680. [\[CrossRef\]](#)
29. Masone, A.; Poikonen, S.; Golden, B.L. The Multivisit Drone Routing Problem with Edge Launches: An Iterative Approach with Discrete and Continuous Improvements. *Networks* **2022**, *80*, 193–215. [\[CrossRef\]](#)
30. Najy, W.; Archetti, C.; Diabat, A. Collaborative Truck-and-Drone Delivery for Inventory-Routing Problems. *Transp. Res. Part C Emerg. Technol.* **2023**, *146*, 103791. [\[CrossRef\]](#)
31. Schermer, D.; Moeini, M.; Wendt, O. A Matheuristic for the Vehicle Routing Problem with Drones and Its Variants. *Transp. Res. Part C Emerg. Technol.* **2019**, *106*, 166–204. [\[CrossRef\]](#)
32. Wang, Y.; Wang, Z.; Hu, X.; Xue, G.; Guan, X. Truck-Drone Hybrid Routing Problem with Time-Dependent Road Travel Time. *Transp. Res. Part C Emerg. Technol.* **2022**, *144*, 103901. [\[CrossRef\]](#)
33. Boccia, M.; Mancuso, A.; Masone, A.; Sterle, C. Exact and Heuristic Approaches for the Truck-Drone Team Logistics Problem. *Transp. Res. Part C Emerg. Technol.* **2024**, *165*, 104691. [\[CrossRef\]](#)
34. Stolaroff, J.K.; Samaras, C.; O'Neill, E.R.; Lubers, A.; Mitchell, A.S.; Ceperley, D. Energy use and life cycle greenhouse gas emissions of drones for commercial package delivery. *Nat. Commun.* **2018**, *9*, 409. [\[CrossRef\]](#)
35. Park, J.; Kim, S.; Suh, K. A Comparative Analysis of the Environmental Benefits of Drone-Based Delivery Services in Urban and Rural Areas. *Sustainability* **2018**, *10*, 888. [\[CrossRef\]](#)
36. Yowtak, K.; Imiola, J.; Andrews, M.; Cardillo, K.; Skerlos, S. Comparative Life Cycle Assessment of Unmanned Aerial Vehicles, Internal Combustion Engine Vehicles and Battery Electric Vehicles for Grocery Delivery. *Procedia CIRP* **2020**, *90*, 244–250. [\[CrossRef\]](#)
37. Bian, H.; Tan, Q.; Zhong, S.; Zhang, X. Assessment of UAM and Drone Noise Impact on the Environment Based on Virtual Flights. *Aerospace Sci. Technol.* **2021**, *118*, 106996. [\[CrossRef\]](#)
38. Ramos-Romero, C.; Green, N.; Roberts, S.; Clark, C.; Torija, A.J. Requirements for Drone Operations to Minimise Community Noise Impact. *Int. J. Environ. Res. Public Health* **2022**, *19*, 9299. [\[CrossRef\]](#)
39. Tan, Q.; Bian, H.; Guo, J.; Zhou, P.; Lo, H.K.; Zhong, S.; Zhang, X. Virtual Flight Simulation of Delivery Drone Noise in the Urban Residential Community. *Transp. Res. Part D Transp. Environ.* **2023**, *118*, 103686. [\[CrossRef\]](#)
40. Lieb, T.J.; Treichel, J.; Volkert, A. Noise Measurements of Unmanned Aircraft Vehicles: Experiences, Challenges and Recommendations for Standards Taken from Flight Trials. In Proceedings of the 2023 Integrated Communication, Navigation and Surveillance Conference (ICNS), Herndon, VA, USA, 18–20 April 2023; pp. 1–7. [\[CrossRef\]](#)
41. Zhou, Z.; Brandão, M. Noise and Environmental Justice in Drone Fleet Delivery Paths: A Simulation-Based Audit and Algorithm for Fairer Impact Distribution. In Proceedings of the 2023 IEEE International Conference on Robotics and Automation (ICRA), London, UK, 29 May–2 June 2023; pp. 12052–12057. [\[CrossRef\]](#)
42. Sudbury, A.W.; Hutchinson, E.B. A cost analysis of amazon prime air (drone delivery). *J. Econ. Educ.* **2016**, *16*, 1–12.
43. Choi, Y.; Schonfeld, P.M. Optimization of multi-package drone deliveries considering battery capacity. In Proceedings of the 96th Annual Meeting of the Transportation Research Board, Washington, DC, USA, 8–12 January 2017; pp. 8–12.

44. Chiang, W.C.; Li, Y.; Shang, J.; Urban, T.L. Impact of drone delivery on sustainability and cost: Realizing the UAV potential through vehicle routing optimization. *Appl. Energy* **2019**, *242*, 1164–1175. [CrossRef]
45. Doole, M.; Ellerbroek, J.; Hoekstra, J. Estimation of Traffic Density from Drone-Based Delivery in Very Low Level Urban Airspace. *J. Air Transp. Manag.* **2020**, *88*, 101862. [CrossRef]
46. Moshref-Javadi, M.; Hemmati, A.; Winkenbach, M. A comparative analysis of synchronized truck-and-drone delivery models. *Comput. Ind. Eng.* **2021**, *162*, 107648. [CrossRef]
47. Mathew, N.; Smith, S.L.; Waslander, S.L. Planning paths for package delivery in heterogeneous multirobot teams. *IEEE Trans. Autom. Sci. Eng.* **2015**, *12*, 1298–1308. [CrossRef]
48. Xu, J. *Design Perspectives on Delivery Drones*; RAND: London, UK, 2017. [CrossRef]
49. ISO 14040; Environmental Management—Life Cycle Assessment—Principles and Framework, 2nd ed. International Organization for Standardization: Geneva, Switzerland, 2006. Available online: <https://www.iso.org/obp/ui/#iso:std:iso:14040:ed-2:v1:en> (accessed on 23 August 2024).
50. Yang, L.; Hao, C.; Chai, Y. Life Cycle Assessment of Commercial Delivery Trucks: Diesel, Plug-In Electric, and Battery-Swap Electric. *Sustainability* **2018**, *10*, 4547. [CrossRef]
51. Lee, D.-Y.; Thomas, V.M.; Brown, M.A. Electric Urban Delivery Trucks: Energy Use, Greenhouse Gas Emissions, and Cost-Effectiveness. *Environ. Sci. Technol.* **2013**, *47*, 8022–8030. [CrossRef]
52. Langelaan, J.W.; Schmitz, S.; Palacios, J.; Lorenz, R.D. Energetics of Rotary-Wing Exploration of Titan. In Proceedings of the 2017 IEEE Aerospace Conference, Big Sky, MT, USA, 4–11 March 2017; pp. 1–11. [CrossRef]
53. Zhang, J.; Campbell, J.F.; II, D.C.S.; Hupman, A.C. Energy Consumption Models for Delivery Drones: A Comparison and Assessment. *Transp. Res. Part D Transp. Environ.* **2021**, *90*, 102668. [CrossRef]
54. Fuller, S. Life-cycle cost analysis (LCCA). National Institute of Building Sciences. *Authoritative Source Innov. Solut. Built Environ.* **2010**, *1090*, 1–10.
55. Asiedu, Y.; Gu, P. Product Life Cycle Cost Analysis: State of the Art Review. *Int. J. Prod. Res.* **1998**, *36*, 883–908. [CrossRef]
56. Raghunatha, A.; Lindkvist, E.; Thollander, P.; Hansson, E.; Jonsson, G. Critical Assessment of Emissions, Costs, and Time for Last-Mile Goods Delivery by Drones versus Trucks. *Sci. Rep.* **2023**, *13*, 11814. [CrossRef]
57. Sun, P.; Veelenturf, L.P.; Hewitt, M.; Van Woensel, T. Adaptive Large Neighborhood Search for the Time-Dependent Profitable Pickup and Delivery Problem with Time Windows. *Transp. Res. Part E Logist. Transp. Rev.* **2020**, *138*, 101942. [CrossRef]
58. Bao, D.; Zhou, J.; Zhang, Z.; Chen, Z.; Kang, D. Mixed Fleet Scheduling Method for Airport Ground Service Vehicles under the Trend of Electrification. *J. Air Transp. Manag.* **2023**, *108*, 102379. [CrossRef]
59. Shaw, P. *A New Local Search Algorithm Providing High Quality Solutions to Vehicle Routing Problems*; APES Group, Dept of Computer Science, University of Strathclyde: Glasgow, UK, 1997; p. 46.
60. Chen, C.; Demir, E.; Huang, Y. An Adaptive Large Neighborhood Search Heuristic for the Vehicle Routing Problem with Time Windows and Delivery Robots. *Eur. J. Oper. Res.* **2021**, *294*, 1164–1180. [CrossRef]
61. Solomon, M.M. Algorithms for the vehicle routing and scheduling problems with time window constraints. *Oper. Res.* **1987**, *35*, 254–265. [CrossRef]
62. Uchoa, E.; Pecin, D.; Pessoa, A.; Poggi, M.; Vidal, T.; Subramanian, A. New benchmark instances for the capacitated vehicle routing problem. *Eur. J. Oper. Res.* **2017**, *257*, 845–858. [CrossRef]
63. Krawiec, K.; Dinh, Q.T.; Do, D.D.; Hà, M.H. Ants Can Solve the Parallel Drone Scheduling Traveling Salesman Problem. In Proceedings of the Genetic and Evolutionary Computation Conference, Association for Computing Machinery, New York, NY, USA, 10–14 July 2021; pp. 14–21. [CrossRef]

**Disclaimer/Publisher’s Note:** The statements, opinions and data contained in all publications are solely those of the individual author(s) and contributor(s) and not of MDPI and/or the editor(s). MDPI and/or the editor(s) disclaim responsibility for any injury to people or property resulting from any ideas, methods, instructions or products referred to in the content.